Dynamic channel network extraction from satellite imagery and dynamics of the Jamuna River

Wouter A. Marra

Master of Science in Earth Sciences Thesis

Utrecht 2010

Utrecht University, Faculty of Geosciences

"Whenever (. . .) things seem hard or tough,
Just remember that you're standing on a planet
That's evolving and revolving at 900 miles an hour"

– Eric Idle / Monthy Python, 1983

Dynamic channel network extraction from
satellite imagery and dynamics of the
Jamuna River

W.A. Marra
Student number: 0424013

Supervisors:
dr. M.G. Kleinhans
dr. E.A. Addink

Utrecht University
Faculty of Geosciences
Department of Physical Geography

Final version, December 5, 2010

Universiteit Utrecht

Preface

This thesis is my final work for my Master's degree in Earth Sciences at Utrecht University. The main aim is to individually carry out scientific research and combine a wide scope of academic skills and knowledge of multiple fields.

In this thesis, fields of study beyond Earth Sciences took an important role: besides river morphology, remote sensing and GIS techniques, network analyses methods from neurology became an important part of the methodology. This sheds a whole new light on river network analyses and will hopefully lead to new insights in this field of study.

This Master's research was carried out in the period May 2009 - April 2010, the final version of this thesis was finished in November 2010. This research was supervised by Maarten Kleinhans and Elisabeth Addink.

Acknowledgements

I would like to thank dr. Mamin Sarker for providing the discharge data from the Bahadurabad station and John van Smaalen from ESRI Nederland for providing help with the ArcGIS THIN function. The supporting and critical comments from everyone in the academic group 'River and delta morphodynamics' were quite helpful. Thanks to everybody who provided tips and support for writing this thesis. Special gratitude goes to Eva Lavooi, for thoroughly reviewing an early version of this thesis.

Wouter Marra,
Leeds, November 2010

Abstract

Braiding rivers consist of many channels, separated by bars which split at bifurcations and join in confluences. Much is known about these basic elements and their dynamics. However, the nature, direction and effects of propagation of local changes through the entire channel network has barely been studied and is not fully understood. Logically, the evolution of the river planform is the result of development of the individual elements. The link between the two has not yet been made. In this study, a braided river is considered as a network of bifurcations, confluences and channels. The evolution of the braided river is analysed by considering the river as a network and analyse the development of individual elements in this network.

A novel methodology was developed to extract detailed channel networks of the river form satellite images (not to be confused with hierarchical stream order networks). Both conventional river properties (i.e. braiding index) as properties derived from network analyses were used to analyse the river network evolution. Furthermore, a weighted braiding index is proposed as a measure for the dominance of a channel, this measure is based on the importance of channels which is derived from the network. Besides changes in network properties, the evolution of the channel pattern is analysed by means of the development of individual bifurcations. Bifurcations in the channel networks at two dates are linked by evaluating the similarity in bifurcation configuration. The bifurcation asymmetry is calculated for every bifurcation, the development of bifurcation asymmetry is calculated for every bifurcation linked between two river networks.

The developed methods were designed to be automated and repeatable for the purpose of application to a series of images. These methods were applied to a time series of satellite images of the Jamuna river (Bangladesh) from 1999 - 2004.

The network measure 'betweenness centrality' maps the importance of all elements in the network. These values of importance are calculated from the local channel geometry, but does not directly relate to the local geometry because the whole up- and downstream configuration of the network is taken into account. Other network measures were not directly useful for river network analysis.

An increase of bifurcation asymmetry and a decrease of braiding and weighed braiding index are observed in periods of persistent low discharge and an increase of bifurcation asymmetry and weighed braiding index are observed during high discharge conditions. Due to the large differences in the appearance of the channel pattern during high discharge conditions, the development of bifurcation asymmetry appeared chaotic possibly due to limitation of the current methods used. During the dry season, parts of the river had only one dominant channel, in other words there was no active braiding.

Development of bifurcation asymmetry during persistent low water stages caused the formation of a dominant channel and a decrease of braidingness of the river. During high discharges, abandoned channel are reactivated and discharge is spread more evenly between channels, increasing the braidingness of the river.

The developed methods, especially the network analysis, shows a big potential for river network analysis. The current methods have a few limitations which could be avoided by tailoring the methods more specifically to rivers.

Contents

List of Figures

List of Tables

1 Introduction

1.1 Problem definition

Rivers, even though they all consist of merely water and sediment, occur in many different forms. Rivers may consist of one single or of multiple channels. Individual channels are somewhere between straight, meandering or braided (e.g. *Knighton and Nanson*, 1993; *Leopold and Wollman*, 1957; *Makaske*, 2001; *Nanson and Knighton*, 1996; *Schumm*, 1985). Research has focussed on the distinction between different river and channel patterns and on finding the physical cause for the occurrence of a wide range of patterns (e.g. *Makaske*, 2001; *Nanson and Knighton*, 1996; *Parker*, 1976; *Struiksma et al.*, 1985). Causes and discriminators between different patterns are based on conceptual theories, large datasets of real rivers or experimental channels (e.g. *Jerolmack and Mohrig*, 2007; *Parker*, 1976; *Struiksma et al.*, 1985; *Van den Berg*, 1995). However, the observed pattern is often complex and is always stage-dependant and changes within a season and over time (e.g. *Alabyan and Chalov*, 1998). Research on a smaller scale within a branched river, namely the scale of individual flow bifurcations, shows that bifurcations will become asymmetrical and are inherently instable (*Bolla Pittaluga et al.*, 2003; *Kleinhans et al.*, 2008).

A branched river consists of numerous parallel channels, divided by fluvial bars in braided rivers or floodplains in anastomosing rivers. Channels split at bifurcations and join in confluences. The effect of dynamics of small scale elements in braider river (individual bifurcations, channels and bars) on the evolution of the large scale channel pattern has not been subject to extensive research. It is however logic that the evolution of a channel pattern is the result of processes taking place in the elements of which it consist. Satellite images allows detailed observation of the earth surface and multiple images allows the analysis of the evolution of earth surface processes (fig. 1.1). Remote sensing images, GIS and network analysis allows studying the evolution of a large branched river in terms of the dynamics of individual bifurcations and channel segments. The general aim of this Master's research is as follows:

- To analyse the evolution of a branched river pattern from the behaviour of individual river elements.

1.2 Objectives of this study

With satellite imagery, detailed observations of an area are possible. With remote sensing, the state of a river system can be mapped at a certain moment and changes over time can be mapped by using change detection techniques. In this study, methods including network

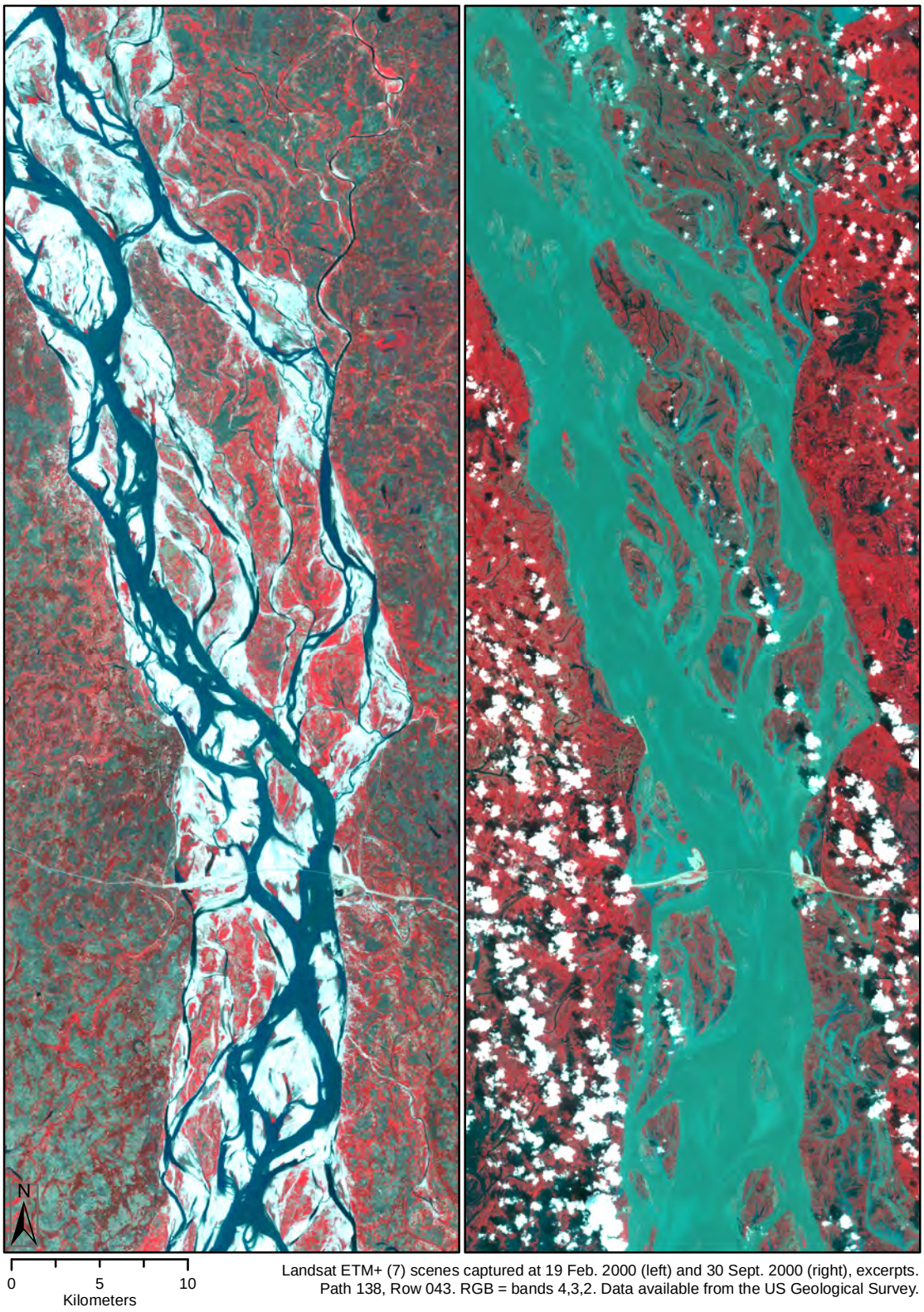

Figure 1.1 Examples satellite images of a part of the research area. The left image shows a scene in the dry season in February 2000, the scene on the right shows the same area with high discharge in September 2000.

analysis are developed to make even more detailed observation of the dynamics in a river. The presence of remote sensing satellites in orbit for over three decades allows observation over a large period of time to assess the evolution of a system. The Brahmaputra / Jamuna is one of Earth's largest rivers and is therefore an interesting study object using satellite images. The large discharge of the river causes morphological processes to happen fast and well observable in a few years. Fluvial processes in the Jamuna occur freely since there are only a few artificial structures in or embanking the river.

In order to test several hypotheses on the evolution of a branched river, quantitative parameters to describe the dynamic behaviour of a river need to be derived from satellite imagery. The dynamics in a river include the development and migration of bifurcations, confluences, channels and bars. To derive such parameters from satellite images, new methods need to be developed which treat the river as a network containing all individual elements: the river pattern can be described as a network of channel segments, bifurcations and confluences. Methods to analyse such network exists, but present techniques are not able to cope with temporal changes in a network. This study has two objectives, one is to develop new methodology and the second is to apply these methods:

- To develop methodology to extract the river channel network from satellite imagery, link the same elements in networks at different dates. This dataset needs to be analysable as network and should thus contain a network topology.
- To characterise and explain the evolution of a branched channel pattern in terms of the dynamics of individual river elements: bifurcations, confluences and channels. Network analysis plays a central role in this analysis.

1.3 Definitions

Different terms are used in different literature for morphological and network elements. In this section, the difference between terms and the used definition in this thesis are given. Terms in bold face are used in this thesis, terms in italic face are terms omitted in this thesis due to possible confusion.

A **branched** river is a collective term for all rivers which have multiple parallel channels. There are two types of branched rivers: braided and anastomosing rivers. In a **braided** river, the river branches within its channel belt and the bars separating the channels are fluvial bars. In an **anastomosing** river, the branches are different channel belts separated by **floodplains**. In an anastomosing river, each channel belt can show a different channel pattern. The term **anabranching** or **branched river** is used for either branched or anastomosing rivers. In a branched river, **channels** split at a **bifurcation** and join in a **confluence** (Fig. 1.2). In this thesis, the term **channel segment** is used for a part of the channel between a bifurcation or confluence and the next one.

The **channel network** refers to the physical network of channels in a branched river. This is different from a *hydrological network* which is the configuration of different order of streams in a drainage basin. The **channel network dataset** is the computer representation of the channel network. In such dataset, the channel segments are represented as **arcs**, and the bifurcations and confluences are represented as **nodes**. The term **object** is used for either nodes or arcs, these are vector representations of physical elements in the river.

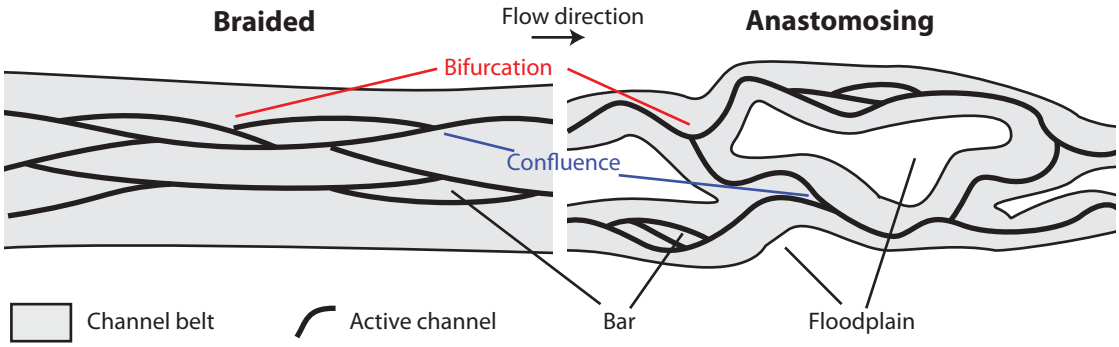

Figure 1.2 Definitions used in braided and anastomosing rivers.

The **logical network** is a set of connectivity information in a network, the connectivity information can be stored in a **connectivity matrix**, which is a data structure. Other data structures can be used to store a network. In network terminology, the nodes are also referred to as *junctions*, but this term is omitted in this thesis as they are the same as the nodes in the channel network dataset. A logical network has no arcs, the connections between arcs are represented as connections with additional properties rather than a physical line element (an arc). The connection between two nodes is referred to as an **edge** in network terminology. Properties of a connection are represented as the weight of an edge.

Different satellite images are used in this study. A **scene** refers to the earth surface captured in a satellite image. All derivatives of an image are also referred to as a scene as these correspond with the same moment of the same location on Earth.

1.4 Review of river pattern research

Three classical river patterns are recognised: straight, meandering and braided (*Leopold and Wollman*, 1957). Besides these basic patterns, anastomosing rivers exist. In an anastomosing river, multiple individual channel belts exist which are separated by floodplains (*Makaske*, 2001). The individual channel belts can feature different channel patterns. In nature, a wide diversity of channel patterns are observed and the pattern changes when different scales are observed and changes with different water heights. The appearance of a river can be described by identifying the pattern (straight, sinuous or branched) for three structural levels (the valley, the flood channel and the low water channel) (*Alabyan and Chalov*, 1998). These observed patterns are different from the three different river types, which have distinct fluvial origins. Discrimination between river types, mainly the transition from meandering to braided, has been made based on empirical relations (e.g. *Ferguson*, 1987; *Van den Berg*, 1995) or the theoretical stability of bar modes (e.g. *Parker*, 1976; *Struiksma and Klaassen*, 1988). The Jamuna river is classified as a braided river in the diagram of *Van den Berg* (1995) (Fig. 1.3).

In meandering rivers, a secondary helicoidal flow is present due to the sinuosity of the river. This causes deposition and development of a point bar in the inner bend (*Knighton*, 1984). Meandering is initiated by large scale perturbations which force an initial flow diversion (*Leopold and Wolman*, 1960) or by alternating bars which are the result of large or small perturbations present in the flow (*Struiksma et al.*, 1985). A flow diversion is in fact a large perturbation.

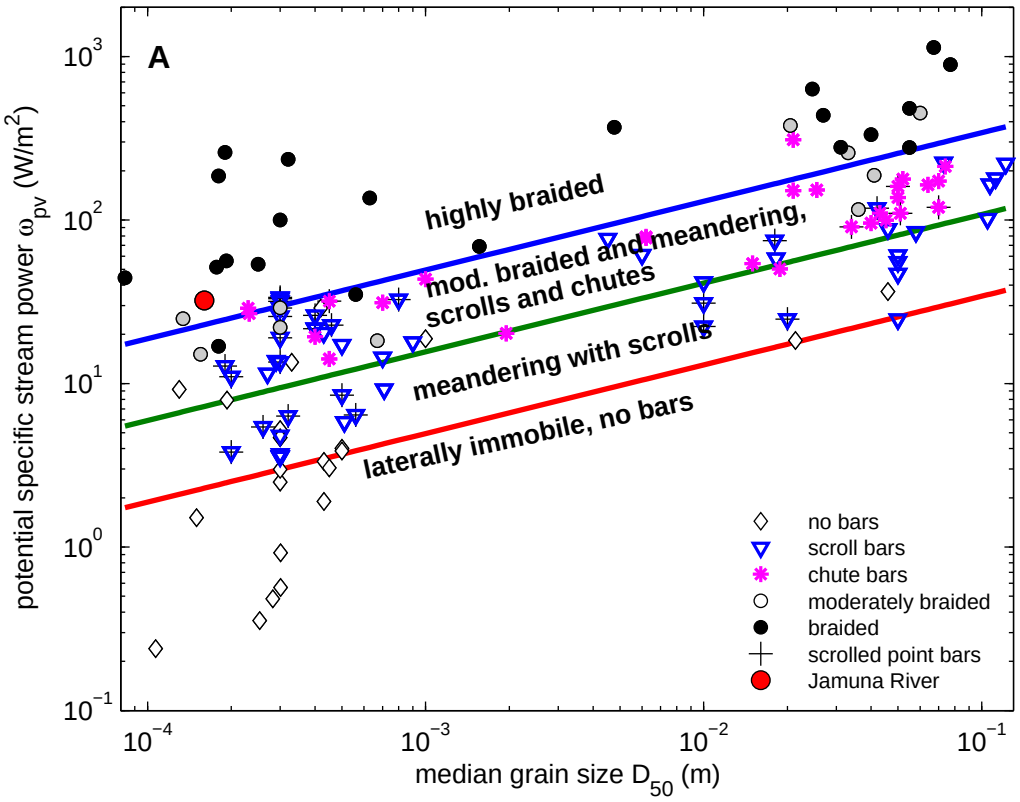

Figure 1.3 Discrimination between different channel patterns, Jamuna highlighted in red, data from: *Kleinhans and van den Berg* (2010). This is an upgraded version of the diagram of *Van den Berg* (1995), the original discriminator between meandering and braided is the blue line.

In braided rivers mid-channel bars exist. The braiding intensity increases with the presence of more mid channel bars and thus more parallel channels. The number of mid channel bars can be predicted by stability analysis from fluid mechanics (*Crosato and Mosselman*, 2009; *Marra*, 2008). As bars do not form above the water table, the braidingness is also a function of water height. Bars can become fixed due to the invasion of vegetation or cohesive sediment. Unsubmerged bars fixed by vegetation can be considered as floodplain as they are no longer subject to migration by fluvial processes. At a bar, the flow bifurcates. Due to the inherent instability of a bifurcation, the bifurcation will become asymmetrical and eventually one of the two downstream channels will close down under constant flow conditions (*Bolla Pittaluga et al.*, 2003; *Kleinhans et al.*, 2008).

Anastomosing rivers remain in existence when the rate of avulsions is equal or higher than the rate of channel closures. Due to the instability of bifurcations, channel closures will always occur and anastomosis is therefore always a dynamic equilibrium. Avulsions occur in aggradating rivers when the in-channel deposition causes the channel to be elevated and a more efficient route of the river is possible (*Makaske*, 2001; *Nanson and Knighton*, 1996). *Huang et al.* (2004) explained the exitance of multiple channels using a sediment transport optimisation theory, in their theory it is more efficient for a river with a high sediment load to transport the sediment over two or more channels. This theory is not compatible with the observation of bifurcations instability. The number of channels in a river will tend to reduce to one due to the instability of bifurcations. A physically sound cause for the presence of multiple parallel channels is therefore yet to be found.

1.5 Review of network analysis

A braided or anabranching river can be described as a geometric network, a representation of a system with interconnected elements. In this section, a review of how such data structures are organised is presented. Note that a network of a branched river is different than the use of hierarchical stream order networks, which is used to describe the structure of hydrological catchments.

Most applied network analysis emphasises on complex neural, social or service networks and deals with answering questions about shortest distances, connectivity and network optimisation (e.g. *Fletcher*, 1987; *Newman*, 2008; *Strogatz*, 2001). Network representations of the network of a basin have been proposed (*Nikora and Sapozhnikov*, 1993), but these do not deal with the evolution of the network. In view of river dynamics, the temporal change of the network should be considered. A network representation of an experimental braided river was used by *Bertoldi et al.* (2009a). In their study, this representation was made manual from photographs and was used to distinct between active and inactive channels.

1.5.1 Network concepts and structure

Topological analysis and therefore network analysis originated in the eighteenth century when *Leonhard Euler* (1741) proved that the mathematical problem 'The Seven Bridges of Königsberg' had no solution by using a topological representation of the problem. The use of topological representation and network structures has been widely used in mathematics and have proven to be an indispensable tool in understanding complex networks which were elsewise not understandable. Most notable complex networks are the world

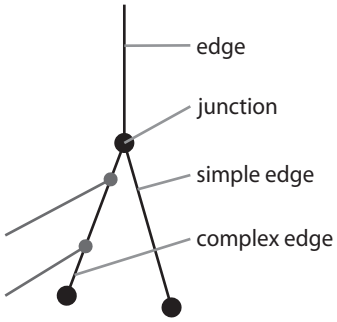

Figure 1.4 Network topology. Edges are connected at nodes, simple edges are connected at two nodes, complex edges have additional secondary edges connected.

wide web, social networks and neurological networks. The basic form of a network is simple: a network consist of nodes and edges connecting the nodes. A network can be either weighted or unweighed when there are or are no weight attached to edges which represent the strength of a connection. A network is directed when there are (flow) directions applied to edges and is undirected otherwise (*Newman*, 2008).

There are two types of edges: simple edges and complex edges. A simple edge is always connected to two nodes, one at each end. A complex edge is connected to two nodes at both ends but can be connected to additional nodes along their length (Fig 1.4). Complex edges should be used when two systems are connected, for example when a highway and a regular road are connected: the highway does not end or split at the node but there is a possibility to switch roads.

The analyses of networks deals with different aspects of networks (see *Strogatz*, 2001, for review). For example: The structural complexity of a network, the evolution of a network over time, complex and diverse types of nodes and edges (e.g. partly connected highway junctions, roads for bicycles only), the influence of one network element to another (e.g. the activation of traffic sign (nodes) by sensors in the road (edge)), and many more. In transportation network analyses, choices of the users of the network (e.g. car drivers) play a role and can be influenced by network properties (e.g. traffic sign settings).

1.5.2 Network structure of a branched river

A branched river consists of multiple parallel channels which join at confluences and split at bifurcations. More generally, a river consists of two types of elements: channel segment and nodes (bifurcations and confluences). A large amount of nodes exist in a braided river and water flows through a large number of channel segments. The number of connections to one node is in most cases limited to two or three and the river flows in one direction (tidal influences in some cases ignored).

All elements in a braided river are affected by other elements, both up- and downstream. The discharge is affected when there is a change in discharge distribution of a bifurcation upstream or by the formation of a new confluence upstream. Due to the backwater effect, the water table is affected by changes in water table downstream. This can affect the distribution of discharge at a bifurcation. In addition, the elements in a river network are dynamic: the properties of an edge can change over time and edges can appear

or disappear.

These natural characteristics of a river can be represented in a dataset containing a network topology. Such dataset allows the analysis of elements in the river with respect to up- and downstream elements due to the presence of connectivity information. In a river, bifurcations and confluences can be represented in a network as nodes and the channels as edges. Each edge may have a set of properties, like the channel geometry. Such properties can be used in the analysis of the network. In a river network, most edges are simple edges since water can move freely along the flow direction, as long as no artificial structures like sluices are present.

1.6 Gaps in knowledge

The processes causing different channel patterns are studied extensively. The development of single bifurcations has also been studied in detail. In braided and anastomosing rivers, these two fields of study unite: branched rivers consist of multiple channels and of numerous bifurcations and confluences. The evolution of a branched river is to a large extent the result of the development of every single bifurcation. The effect of the development of single bifurcations on the evolution of the river pattern has not been subject to extensive research and leads to the aim of this study: to analyse the evolution of a branched river from the behaviour of individual elements.

In order to analyse the evolution of a river in this way, temporal information of a river is needed. Also, sophisticated methods to deal with a large amount of elements are needed. Remote sensing and satellite imagery offers great opportunities to obtain a dataset of a large river over a period of time. Network representations and network analysis offers methods to deal with structures with a large amount of interconnected elements.

1.7 Hypotheses

1.7.1 Evolution of a braided river pattern

A channel with a stable flow has a steady state configuration in terms of number of channels and nodes (*Bertoldi et al.*, 2009a) or in terms of number of bars per cross section (*Crosato and Mosselman*, 2009; *Marra*, 2008). The number of bars is mainly a function of width to depth ratio, with higher water levels corresponding to the development of more bars per cross section. Bars in channels only form up to the water level (*Parker*, 1976), thus unsubmerged bars are the result of discharge variations (*Marra*, 2008). Furthermore, the observed river pattern changes with different stages (*Alabyan and Chalov*, 1998). On the upstream side of an unsubmerged bar, the flow bifurcates. Bifurcations will become asymmetrical and eventually only one of the channels remains (*Bolla Pittaluga et al.*, 2003; *Kleinhans et al.*, 2008).

The dynamics in a braided river are the result of these processes, both increasing and decreasing the braidingness of the river. The following hypotheses are raised:

1. In a braided river, a dominant channel develops during steady flow conditions. Due to the inherent instability of bifurcations, one of the channels downstream of a bifurcation will grow while the other closes. The formation of such dominant channels will diminish the braidingness of the river.

2. The braided pattern is maintained by frequent flooding. During high flow conditions the observed channel pattern is less braided since smaller bars are submerged; but bars are created or activated under the water level and abandoned channels are reactivated, counteracting the bifurcation asymmetry generated during steady flow conditions.

The first hypothesis can be tested by mapping the temporal development of the channel network of a braided river. If for a significant amount of the bifurcations one of the downstream channel will become dominant during a period of steady flow, this hypothesis is considered proved. A measure of the development of bifurcation asymmetry needs to be derived from the changes in the river network.

The latter hypothesis can be tested by considering the channel pattern under the same flow conditions before and after a flood event. The braidingness is expected to be lower during- and higher after an event with high water stages. An inverse correlation between stage and braiding index with hysteresis is expected.

1.7.2 Network analysis in braided rivers

Geometrical network analysis has previously not been used to describe the behaviour of a river. However, a branched river appears as a network and thus a network representation can be created and analysed. Methods exist for the extraction of river channels and basic channel properties from satellite images (e.g. *Jagers*, 2003). Besides the representation of the river as a network, the evolution of the geometric network should be considered. Based on available GIS procedures, such analysis seems possible. The following hypotheses are raised:

3. A geometric network representation of a braided/branched river can be extracted from satellite images. Qualitative analysis on the evolution of a river can be performed using this representation and additional channel properties derived from the satellite image.

4. Multiple scenes of the same river at different dates can be linked. This yields a dataset which can be used to assess changes of objects in the channel network.

Different approaches and techniques are tried, aiming at the development of a generally applicable method which is useable and valuable in studies of other branched rivers and other (hydrological) networks.

1.8 Study area

In order to use satellite images for analysing the evolution of the channel pattern, a large river is needed. The Brahmaputra is one of the largest braided rivers in the world and suited for this research. The Brahmaputra flows through China (Tibet), India and Bangladesh; the study area is located in Bangladesh (Fig 1.5). The Brahmaputra river splits near Gaibanda ($89°32'47''E$, $25°19'32''N$) into the relative small Old Bramahputra and the Jamuna River, which is the major course of the Brahmaputra River nowadays. This point is taken as the northernmost boundary of the study area. Also, at approximately this location, Landsat satellite images are cut. The Jamuna River flows almost straight south

to the confluence with the Ganges rives near Rajbari ($89°39'6''E$, $23°45'14''N$), from here the river is called the Padma River. This confluence is the southernmost boundary of the study area.

The Jamuna has a yearly flood in July-August, the average flood has a discharge of $60 \cdot 10^4\ m^3s^{-1}$. The lowest discharges are about $0.5 \cdot 10^4\ m^3s^{-1}$, these are measured in January until February. In this period the discharge is fairly constant. Discharges gradually increase from March until June and decrease gradually from September until December.

The study area could be expanded towards the north since the Landsat satellites make a south-to-north overpass and the scene north of the scene of the current study area is acquired in the same orbit. However, for a large part of the available scenes, the northern counterpart is not available.

1.9 Structure of this thesis

First, available conventional methods are described (Chapter 2), this is the basis of newly developed methods (Chapter 3). Then, an interpretation of the results of these methods and meaning in terms of river evolution are presented (Chapter 4). The reliability and applicability of the developed methods and the results are discussed (Chapter 5), followed by conclusions (Chapter 6). Finally, thoughts for future research are presented (Chapter 7).

The used and created data and all the developed methods (scripts) for the research of this thesis is available on a hard disk, contact the author or one of the supervisors if this data is required. The general data structure of this disk is described in Appendix A.

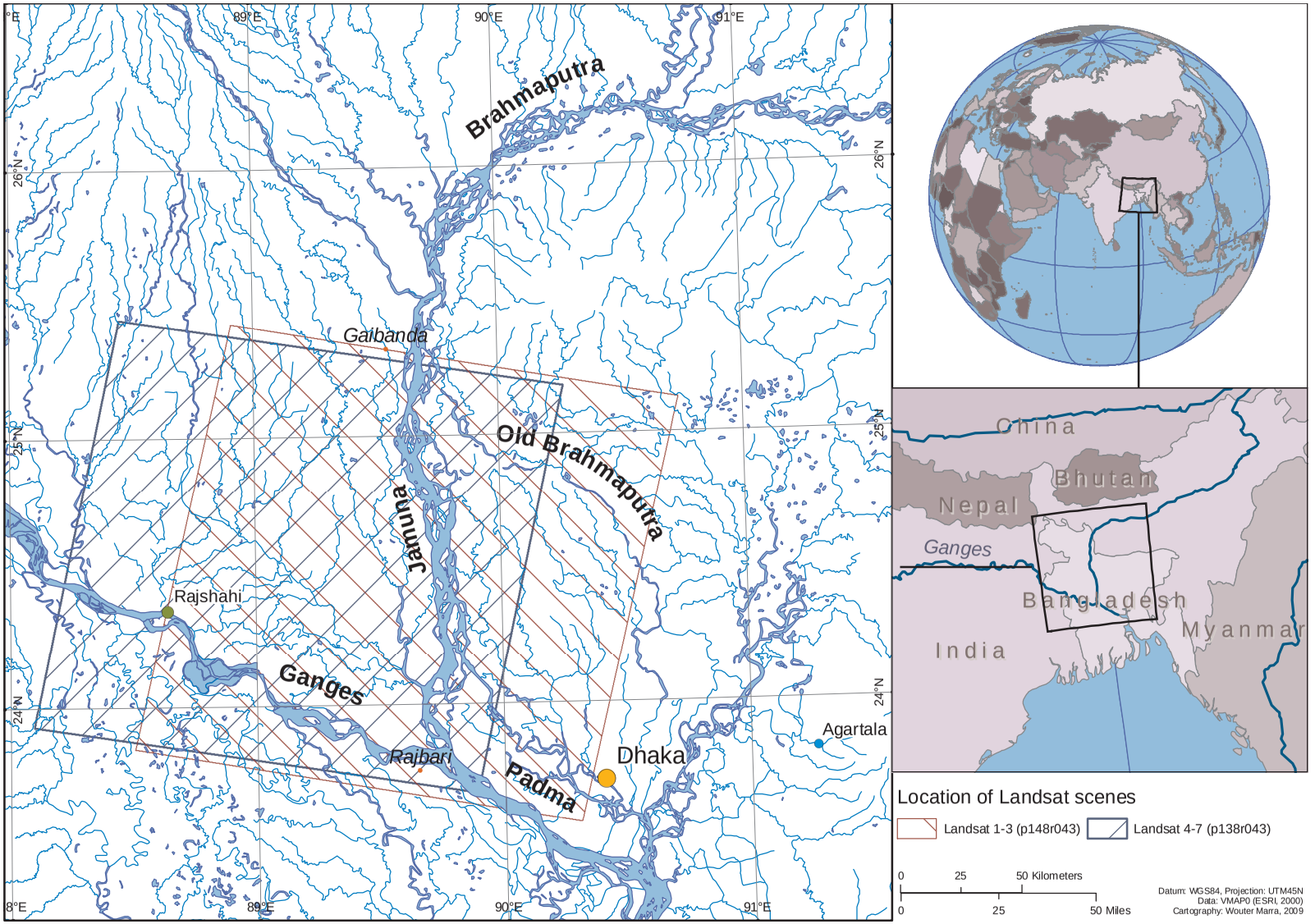

Figure 1.5 Overview of the study area

2 Methodology and data

In this chapter, the available methods and data are described. Newly developed methods are presented in the next chapter (Chapter 3). The used data are satellite images and discharge data, available methods for processing and classification of satellite images are given. The concept of network analysis and available network measures are given. Finally, the used concept for the calculation of braiding index is given.

2.1 Satellite images and image classification

The basis of the data used were satellite images of the study area. From classified satellite images, the river network was extracted. Available classification techniques are described in this chapter. The developed method to extract the river network is the scope of Chapter 3.

2.1.1 Data

Satellite images from the Landsat platform were used. This platform offers a high spatial resolution (up to 30 m), and most of the data is freely available (*USGS*, 2008). A selection of Landsat scenes based on scene cloud cover and overall quality was used (see Tab. 2.1). All scenes used are either captured with a TM or ETM+ sensor and have a resolution of 30 m. A large data gap exists for the study area from 1980 until 1989 and from 1991 until 1999. In the selected scenes, there are two series of successive satellite images (November 1999 – September 2000 and October 2002 – February 2003) and there are almost yearly images taken in November (1999 – 2002 and 2004). The hydrological situation of the scenes are presented in Figs. 2.1 - 2.2. The images were requested and downloaded from the USGS through their data localisation tool GloVis. All used satellite images are displayed in Appendix D.

2.1.2 Image pre-processing

Satellite imagery (including Landsat data) is typically delivered in calibrated digital numbers (DNs). To ensure consistency between different scenes, these DNs need to be converted to reflectance. Inconsistency between scenes is the result of different sensitivity to incoming radiance of different sensors and due to differences in scene-to-scene exo-atmospheric solar irradiance. DNs were converted to at-sensor radiance by applying a sensor-specific calibration function (Eq. 2.1, *Chander et al.* (2009)):

$$L_\lambda = \left(\frac{LMAX_\lambda - LMIN_\lambda}{Q_{calmax} - Q_{calmin}} \right) (Q_{cal} - Q_{calmin} + LMIN_\lambda) \tag{2.1}$$

Table 2.1 List of used Landsat scenes. Dates marked with * are all scenes in the same time of the season (Fig. 2.1). Dates marked with [1] and [2] denote two contiguous periods (Fig. 2.2 and Fig. 2.3, respectively). Selection of scenes was made on atmospheric conditions.

Date (yyyymmdd)	Landsat Scene Identifier	Sensor
19991112 [1,*]	LE71380431999319SGS00	ETM+
20000203 [1]	LE71380432000034SGS00	ETM+
20000219 [1]	LE71380432000050SGS00	ETM+
20000509 [1]	LE71380432000130SGS00	ETM+
20000930 [1]	LE71380432000274SGS00	ETM+
20001117 *	LE71380432000322SGS00	ETM+
20011120 *	LE71380432001324SGS00	ETM+
20021006 [2]	LE71380432002279SGS00	ETM+
20020224 [2]	LE71380432002055SGS00	ETM+
20021123 [2,*]	LE71380432002327SGS00	ETM+
20030126 [2]	LE71380432003026SGS00	ETM+
20030227 [2]	LE71380432003058SGS00	ETM+
20041104 *	LT51380432004309BKT00	TM

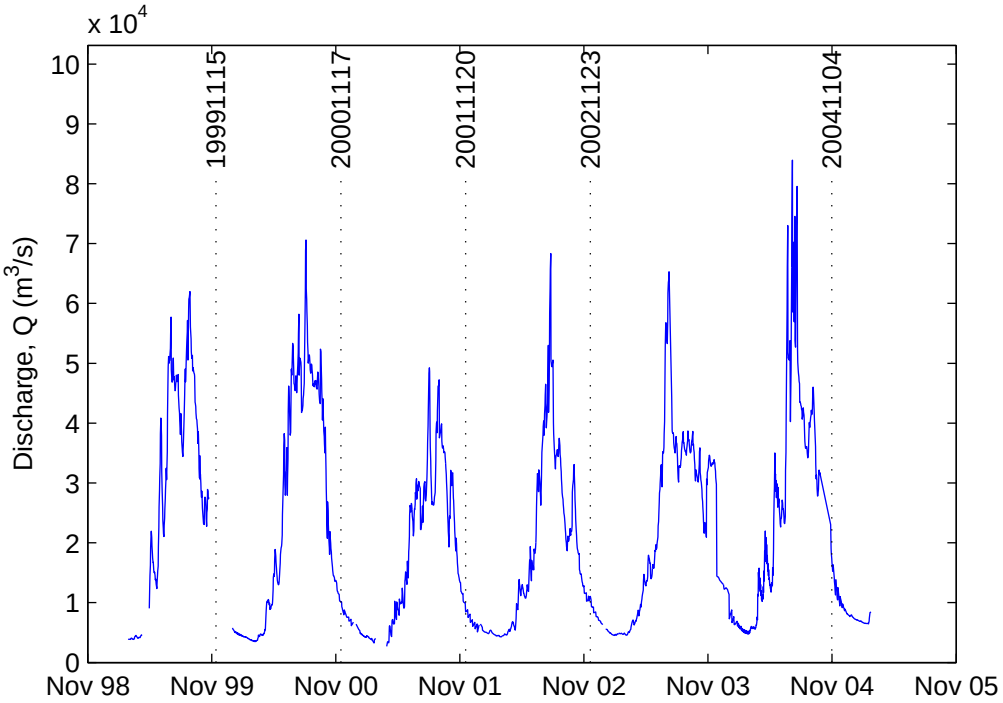

Figure 2.1 Hydrograph at Bahadurabad for 1998 - 2005

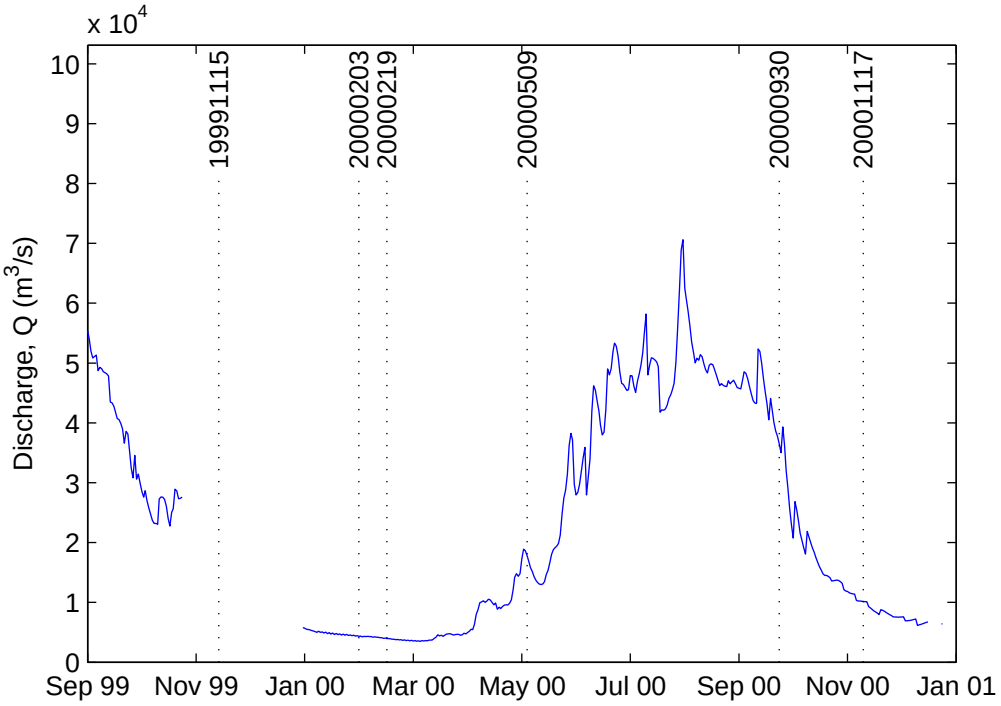

Figure 2.2 Hydrograph at Bahadurabad for 1999 - 2001

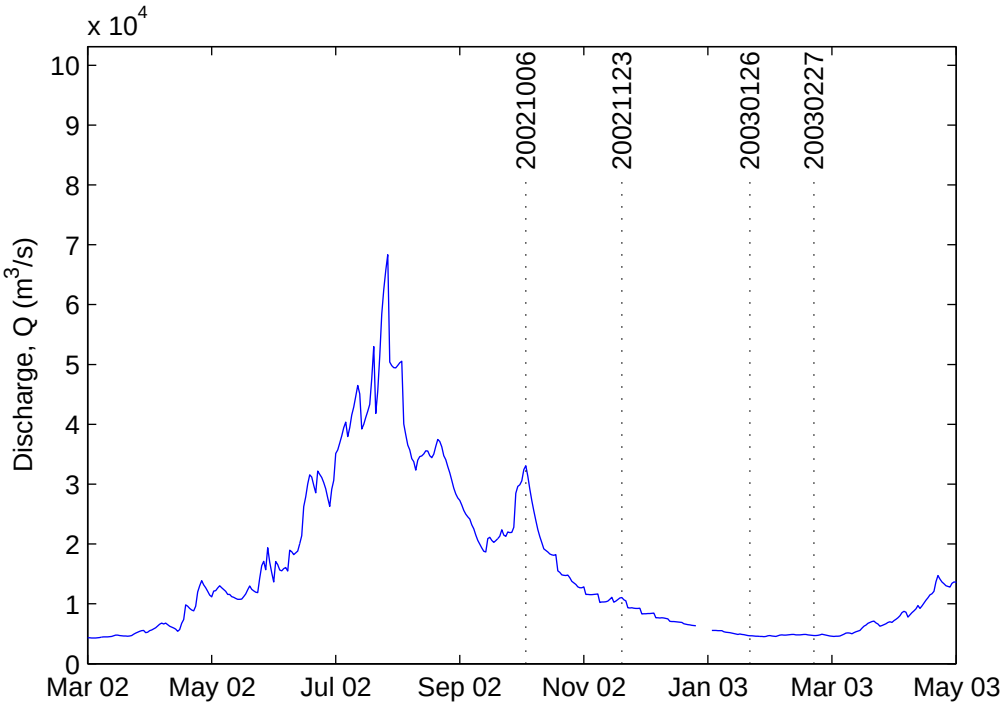

Figure 2.3 Hydrograph at Bahadurabad for 2002 - 2003

where L_λ is the spectral radiance at the sensor $(W/(m^2\ sr\ \mu m))$, Q_{cal} is the calibrated pixel value (DN), Q_{calmin} and Q_{calmax} are the minimum and maximum pixel values, corresponding to $LMIN_\lambda$ and $LMAX_\lambda$ which are the spectral radiance for these DNs at the sensor $(W/(m\ sr\ \mu m))$. Calibration data for all Landsat sensors are available in *Chander et al.* (2009) and is provided in the meta data of Landsat data files. The usage of calibration data provided with the Landsat data is preferred since the sensor performance changes over time.

At-sensor radiance changes due to changing solar irradiance and atmospheric conditions causing scene-to-scene variations. In order to compare different scenes, radiance data was transformed to reflectance. Ideally, to compare surface scenes, surface reflectance is preferred. Since atmospheric conditions are not exactly known, usually no atmospheric corrections are applied. Reflectance scenes considering only the solar irradiance are referred to as top-of-atmosphere (TOA) reflectance. The calculation includes seasonal variation in exo-atmospheric solar irradiance due to differences in earth-sun distance and variation in solar zenith angle (Eq. 2.2).

$$\rho_\lambda = \frac{\pi \cdot L_\lambda \cdot d^2}{ESUN_\lambda \cdot \cos\theta_s} \tag{2.2}$$

where ρ_λ is the TOA reflectance $(-)$, L_λ is the spectral radiance at the sensor $(W/(m^2\ sr\ \mu m))$, d is the earth-sun distance (*astronomical units*), $ESUN_\lambda$ is the mean exo-atmospheric solar irradiance for the specific band $(W/(m^2\ \mu m))$ and θ_s is the solar zenith angle during acquisition of the scene $(degrees)$. Earth-sun distance was calculated using an astronomical model. The mean exo-atmospheric solar irradiance is sensor specific (values available in *Chander et al.* (2009)). The solar zenith is a function of location at the earth and time. The cosine of the solar zenith is equal to the sine of the solar elevation angle, which is provided in the meta data of Landsat data files.

All data were radiometrically calibrated and converted to top-of-atmosphere reflectance values in order to correct for seasonal and scene-to-scene variations in solar irradiance. The reflectance data was used for further processing. An automated script in the programming language Python in combination with ArcGIS geoprocessing scripts for Python (Python version 2.5.1 and ArcGIS version 9.3.1 with spatial analyst extension) was created to calibrate the data (scripts available on accompanying hard disk, see Appendix A).

2.1.3 Image classification

The satellite images were classified in order to separate the river from other objects in the scene. The images consist of a few well-separable main classes: water, vegetation, sand and – in some images – clouds.

To extract these features more easily from the image, a Tasselled Cap transformation was applied to the images. This resulted in a 3-band image, the bands represent brightness, greenness and wetness (*Lillesand et al.*, 2007, §7.6). The transformation was applied to reflectance data images (transformation coefficients from *Crist* (1985) (TM-sensor images) and *Huang et al.* (2002) (ETM+-sensor images)).

The required classes are well separable in the resulting Tasselled Cap images feature space. The images were classified using a supervised classification with non-parametric signatures. In other words, these images were classified by delineating pixel clusters in

the feature space. This process resulted in classification signatures with no mixed pixels, as no overlapping signatures were created. Pixels outside the defined signatures were left unclassified and were then assigned the nearest neighbour classified pixel afterwards. This was done to prevent wet-vegetation pixels to become classified as water when there is no water surrounding. Images with comparable conditions taken in the same period of the season were classified using the same signature sets. Image transformation and classification was performed in ERDAS IMAGINE (version 9.2). All classified images are available in Appendix E.

2.2 Network analysis

In this section the possibilities of analysing a branched river as a network are described. A review about network concepts and the network structure of a branched river are given in Section 1.5. To summarise: a branched river can be represented as a network with confluences and bifurcations as nodes and the connected channels as connecting edges. This network is directed and various weights representing channel geometry can be applied to the edges.

2.2.1 Network measures

A network can be mathematically analysed. Network analysis is widely used in social network and neurological studies, fields of science where has to be dealt with large and complex networks. Network measures can give valuable insight in the state and behaviour of river networks.

Different descriptive or statistical parameters of a network can quantify the properties of the network, or a part of the network. Numerous parameters exist, some far more complex than others. Inhere, some basic network properties are presented, all of which are available in the Brain Connectivity Toolbox (BCT) (see *Rubinov and Sporns*, 2009, and Fig. 2.4). These measures originated in various fields of science, and were all found to be useful in Neurological science. This specific toolbox is used as it provides relative easy out-of-the-box network analysis. Possible limitations of using a neurology based toolbox for river network analysis is discussed later. These network measures were calculated for all river networks extracted and analysed whether useful as morphological measures. The BCT is a set of functions in MATLAB. Calculations are available in *Rubinov and Sporns* (2009), and were performed in MATLAB (version: 7.9.0.529; R2009b).

The **degree** of a node is the number of edges connected to that node. The degree distribution of a network gives insight in how the network is organised. For many networks, the degree distribution is a power function: only a small number of nodes have a large amount of connected edged and the largest part of the nodes have a small amount of connected edges (*Newman*, 2008; *Sporns*, 2002). In a directed network, there is a difference between incoming and outgoing edges, the indegree and outdegree.

The **strength** of a node is the sum of the weights of the connected edges. In a directed network, there is an inweigth and outweight, the sum of weights of all incoming or outgoing connections (*Barrat et al.*, 2004).

The importance of a node can be addressed by the **centrality** of a node (*Freeman*, 1987). The **betweenness centrality** of a node is the fraction of all possible shortest paths between

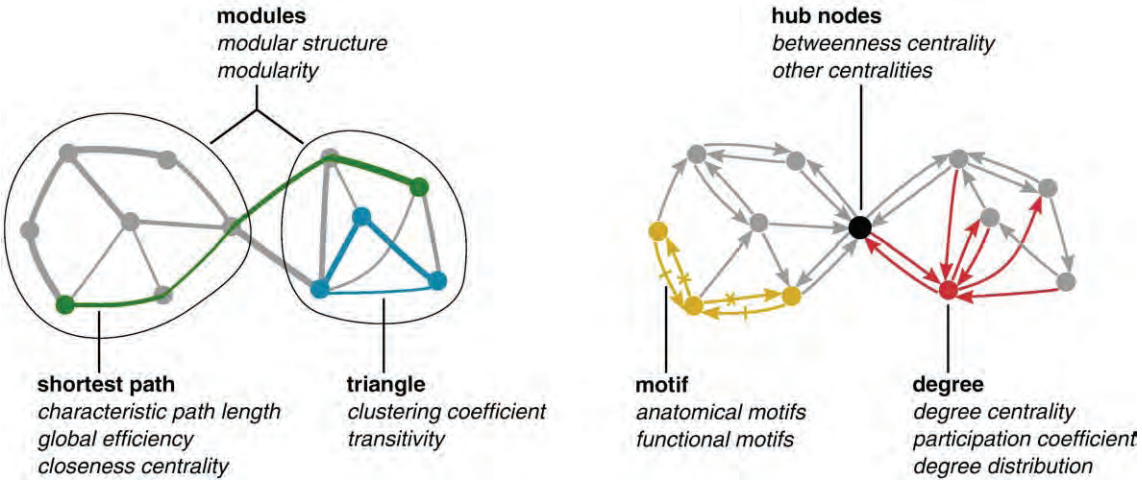

Figure 2.4 Measures of network topology, from: *Rubinov and Sporns* (2009). Bold type indicates basic network properties, italic type indicates complex network measures described in *Rubinov and Sporns* (2009).

nodes in the network that pass through that specific node. Weights and directions of edges are used in calculating the shortest paths. The weight of an edge is considered as the distance between two nodes, higher weights denote a shorter distance. The weight is not necessarily the physical distance between two nodes, but could represent the strength of a connection (as used in neurology) or the width in the case of rivers or a combination of different properties.

A measure of the interconnectedness or segregation of nodes is the **clustering coefficient**. The clustering coefficient indicates how many direct neighbour nodes of a node are connected to each other.

The **assortativity** is the correlation between the degree of a node and the degree of the linked nodes. A high assortativity indicates that nodes with many connections are also connected to nodes with many connection and nodes with a small number of connections are linked to other nodes with a small number of connections (*Newman*, 2003).

The **modularity** is a measure for the presence of distinct communities in a network. A **community** is a cluster of nodes which are highly connected to each other, compared to other nodes in the network (*Newman*, 2006).

In river morphology, the braiding index can be considered as a network property as well. In network terms, it describes the average number of parallel edges. Such index ('parallelness') is only derivable when the network has spatial coordinates.

2.3 Accompanying methods

In order to interpret network measures, the results from the developed methods were compared to conventional data describing the river. The data was compared to visual interpretation of the satellite image, to discharge data and the braiding index. The location of the extracted channels were compared to the satellite image in order to validate the location of the the channel and to check whether the extracted channels are not interrupted when the channel in the satellite image is.

The discharge data was used to help the interpretation of the results. Discharge data

gives insight in the conditions at the moment of the satellite image and the conditions between two images, especially the presence (or absence) of discharge peaks is important. Daily discharge data at the Bahadurabad gauging station since 1954 was used (from unpublished governmental report).

2.3.1 Braiding index

The braiding index is a measure for the number of parallel channels per river cross section. Various calculation methods exist, of which every variant is affected and influenced in its own way (see *Bridge*, 1993; *Egozi and Ashmore*, 2008, for review). The best method, having the least influence of channel angles and stages, as proposed by *Egozi and Ashmore* (2008) was used. This method is also one of the most simplest: a simple count of the number of parallel channels per cross section. Because the river channel network is presented in as a digital GIS dataset, this calculation was done automatically. Furthermore, the braiding index was calculated as a variable along the river. This gives insight in the changes in different segments of the river

3 Developed methodology

In this chapter, the developed methods to create and analyse the river network are described. First, the process of extracting the river channels from a classified image is described. Then the process of converting the river channel dataset into a network dataset is explained. The calculation of network measures and derivatives of network measures are described. Then, in order to assess the development of the river, methods are described to link two networks at different dates and analyse the development of individual bifurcations. In the last section a new measure, the weighted braiding index, is proposed.

3.1 River channel extraction

In this section, the developed methods to extract river channels from a classified satellite image are described. The river channel network was extracted from a classified image with at least the land cover class 'water'. Additionally, the width of the channel was added to the river network in order to make more advanced analyses.

The used workflow was as follows (see Fig. 3.1, explained in more detail in the next sections): From the classified image all river pixel and non-river pixels were selected. From the river pixels the channel centrelines were extracted. The width of the channels were derived from the data and were added to the dataset. The width is twice the distance to the nearest non-river pixel at the centre of the channel. The final product of this procedure is a dataset of the river channels, consisting of arcs and nodes (ArcGIS Coverage format). This data type is preferred since a correct topology is instrumental in creating a network network topology.

The river network extraction described here was performed in ESRI ArcGIS (licence: ArcInfo, version: 9.3.1 SP1, build 3500) with the Spatial Analyst extension and Coverage Toolbox (the latter is available with ArcInfo Workstation). Scripts and created data are available on the accompanying hard disk, see Appendix A. All extracted centrelines are available in Appendix F.

There is a key difference in topology in the dataset containing the channels of the river network and the topology of a logical network. In a standard geographic topology (as produces by ArcGIS), for every arc the nodes to which it is connected are known. In a network topology, for every node the nodes and arcs to which it is connected are known. In order to analyse the network, a network topology was build from the river channels dataset, which has a standard vector topology.

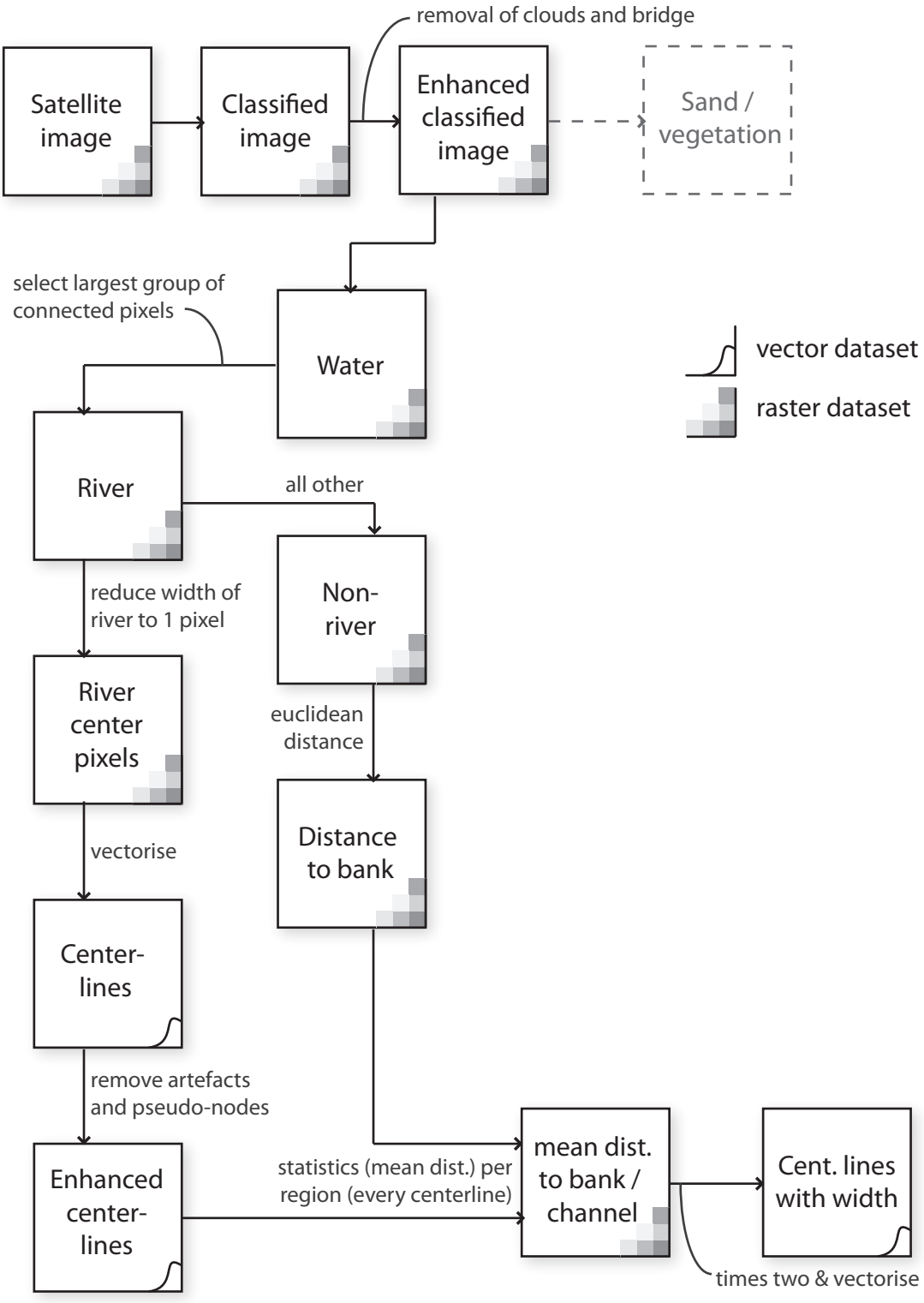

Figure 3.1 Flow chart of the extraction of the river channel network from satellite images

3.1.1 Selection of river channel pixels from classified image

In this section, the procedure to select the actual river from the satellite image is explained. First, the classified image needs enhancement, mainly due to the following three effects: 1) Some classified images contain a cloud class besides the desired classes. 2) In the current study area a bridge is present, interrupting the river. 3) Edges of classes are often frayed due to spectral mixing.

The clouds and the bridge were removed from the image by nearest-neighbor interpolation within these areas. For the bridge, an interpolation mask containing only the pixels of the bridge was created and was used for every classified image. For all images containing clouds, the clouds were selected from the classified image. This selection was then used as an interpolation mask. Unfraying class edges was performed after the river pixels were identified from the image to prevent interference with that process.

From the cloud- and bridge-free image only the water pixels were selected. This selection contains both river as non-river water pixels. In the used images, the river is by far the largest water body in the image, making the selection of the river possible using the following procedure. 1) Every cluster of pixels were assigned to unique groups: vertically, horizontally and diagonally connected pixels were considered in the same group. 2) For every unique group the surface area was calculated. 3) All pixels containing the maximum value were identified as river pixels.

The resulting river class often had frayed edges. Such edges would result in individual channels in the channel extraction process and need to be removed. This was done by subsequently expanding and shrinking the river class pixels one pixel. This process removes bulges and holes in the river class of only one or two pixels. Also, non-water areas of only one pixel wide inside the water class are removed by this process.

A vast majority of all small non-water areas within the water class are not bars, but classification errors. These errors are mostly induced by high concentration of sediment causing the spectral reflection to be more like sand than water. These small areas were selected by a similar process as the selection of river pixels from the water pixels. 1) Every cluster of non-water pixels were assigned to unique groups but only vertically and horizontally connected pixels were considered in the same group. 2) For every group the area was calculated. 3) All pixels of groups with an area smaller than 21600 m^2 (24 pixels) were removed from the non-river class and added to the river class. The value of 24 pixels is the result of trial and error, for the current research area this value corresponds with tiny objects (24 pixels equals about $1.7 \cdot 10^{-4}$% of a 14-Mpixel Landsat 5 or 7 image).

3.1.2 Centreline extraction

Vector centrelines of the river pixels were extracted in order to make a network representation. First, centre pixels of the river class were extracted, this process introduced some artifacts which were removed. Then the centre pixels were vectorised. The resulting centrelines still contained errors which were removed manually.

A thinning algorithm was used to get the centre pixels of the river class. This algorithm reduced the number of cells representing the river, while retaining its structure. This resulted in a one-cell wide skeleton of centre pixels.

The thinning algorithm produces different types of errors: 1) small artifacts at locations with small channel width variations, 2) the introduction of 'centrelines' perpendic-

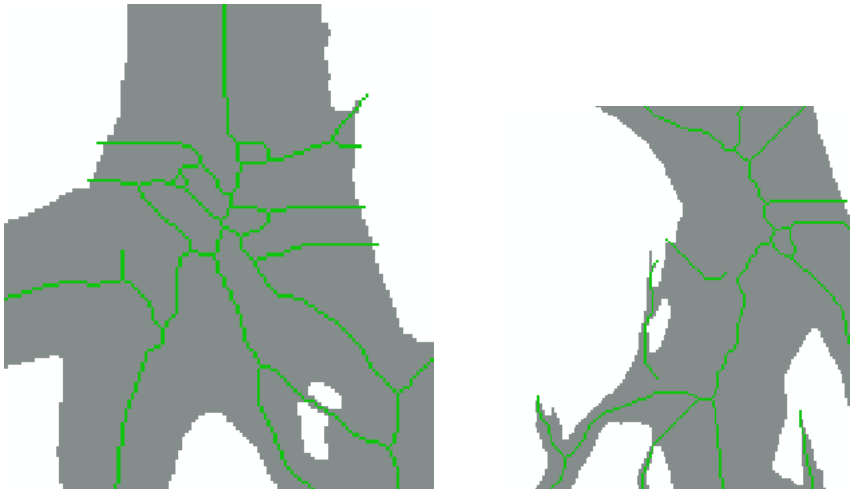

(a) Artifacts and channel segment perpendicular to the channel

(b) Unconnected channel segments

Figure 3.2 Errors introduced by centrepixel selection algorithm

ular to the real centreline in wide channels with an irregularity in channel width and 3) unconnected channel segments (Fig. 3.2b). The first error was filtered, the second was removed in the conversion to vectors and the third was corrected manually:

- Small artifacts, consisting of one or two pixels were removed by expanding the centrepixels by two pixels and performing the thinning algorithm again (Fig. 3.3). This process does not introduces new errors since all centre pixels are always spaced more than two pixel from each other.
- The enhanced centre pixels were converted to vector lines. In this process all dangling vectors shorter than 2000 m were discarded (Fig. 3.4). These dangling lines were for the largest part errors introduced by the thinning algorithm. Longer dangling arcs were mostly not the results of errors, but were real non-continuous channel segments.
- The resulting set of centrelines were edited manually. In this process prevailing artifacts were removed, unconnected centrelines which should have been connected were connected and residual unconnected (dangling) channels were removed. For justification of choices, the original satellite image was used as guidance.

For the final product, every channel segment should consist of only one arc. In other words, all nodes must be bifurcations or confluences. During the process various pseudo-nodes were created, these are nodes which have only two arcs connected. These pseudo-nodes were dissolved by aggregating adjacent arcs. The resulting dataset consist of a set of nodes and one arc for every channel segment.

3.1.3 Determination of channel width

The channel width was derived by doubling the distance between a centreline and the nearest bank. The channel width was derived for every channel segment. The process was as follows:

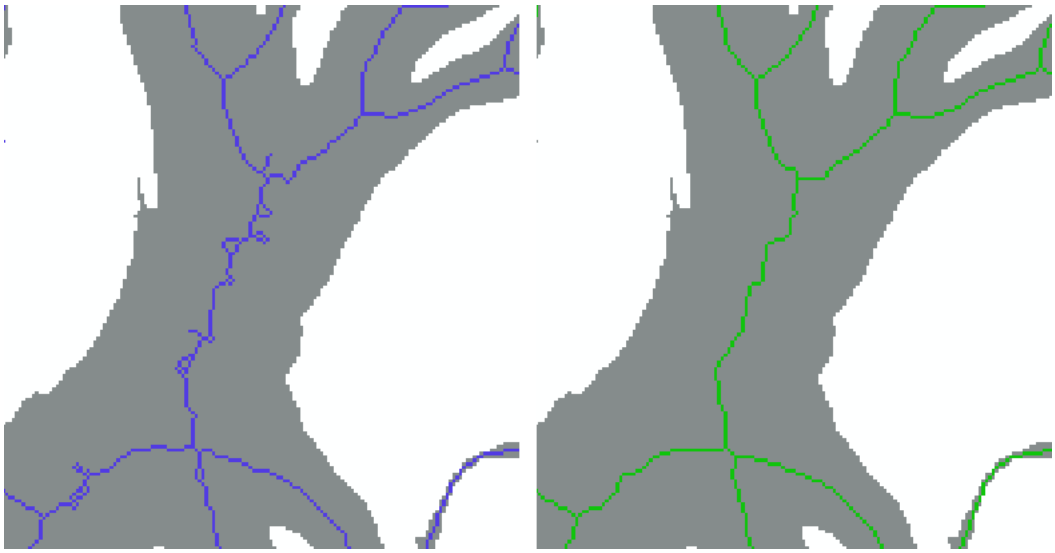

Figure 3.3 Result of enhancement of centrepixel extraction. The left images shows the initial result of centre pixel extraction, the right image is the result of enhancement of the initial centre pixel dataset.

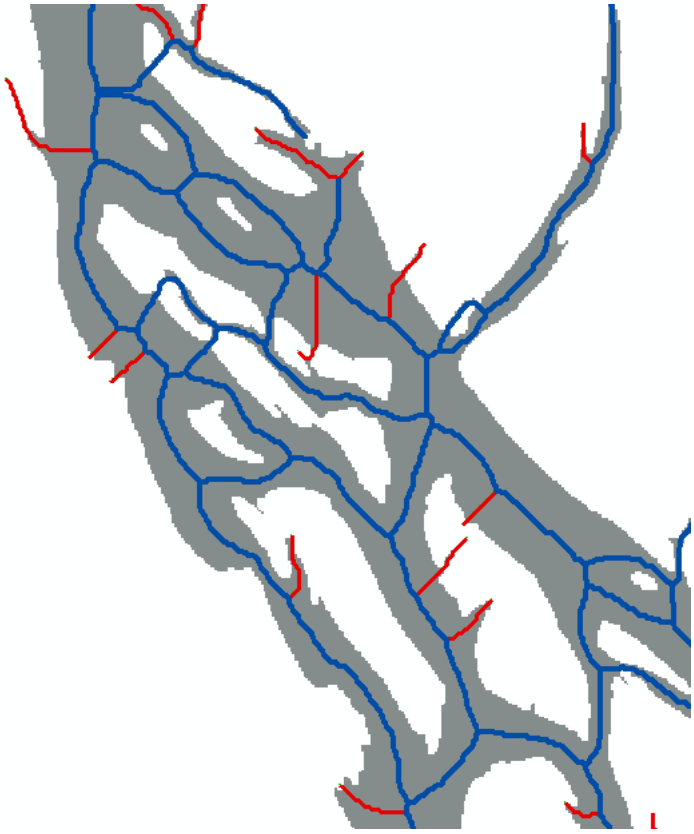

Figure 3.4 Removal of unconnected channels (dangling arcs): red arcs are removed in the process.

- A raster map with the Euclidean distance to the nearest non-water pixel was created and multiplied by two. At the centre of the channel, this value correspond with the channel width. This map was converted to integer values, as this is required by functions used later.
- For every individual segment of the centrelines, the mean pixel values of the distance map were calculated. This resulted in a raster map. This raster map is at some junctions of channels wider than one pixel due to the used algorithm. To prevent the introduction of artifacts, this map was thinned again using the mentioned algorithm. The resulting enhanced centre pixels were vectorised. The same procedure was repeated, but now calculating the standard deviations per channel segment instead of the mean width. Both mean width and standard deviation of the width were combined into one dataset.

A topology was built for the dataset. In this process, arcs were slightly simplified: vertices spaced 90 m or less were combined. An arc attribute table (AAT) and a node attribute table (NAT) were built. The AAT contains information about the connectivity of arcs to nodes (in addition to the width), which is the main input for creating a network dataset. Furthermore, arc lengths are automatically calculated in this process. Node coordinates were added to the NAT. The coordinates of the mid-point of every arc were added to a new point dataset. Finally, these three datasets (arcs, nodes and arc mid-points) were added to a geodatabase in order to exchange the data with other software.

3.2 Network generation

The created river network has a geographic topology (as generated by ArcGIS, see *ESRI* (2008) for description), in which the connected nodes are listed for every arc. For network analyses, the topology needs to have a network topology, in which for every node the connected nodes are listed (see Fig. 3.5). In a network topology, arcs are connections between nodes (known as an 'edge') and the properties of an arcs are listed as a weight of an edge. In addition, an edge may have a direction.

In this section, the applied transformation of a standard vector topology to a network topology is described. This transformation only affects the database structure, the spatial representation of the river remains unaltered.

This process yields two products: 1) a connectivity matrix and 2) an additional node attribute table. In a connectivity matrix rows and columns denote nodes and matrix entries denote links (*Rubinov and Sporns*, 2009). In a weighted network, the value of a matrix entry denotes the weight of the connection. Uses of different weights is discussed in Section 3.2.4. Generation of a network dataset was performed in MATLAB (version: 7.9.0.529; R2009b). Scripts are available on accompanying hard disk, see Appendix A.

3.2.1 Generating the network topology

The attribute tables of the river channel dataset were used for the generation of a network topology. See Table 3.1 for notation and explanation.

From the arc attribute table (AAT) the fields 'ObjectID', 'FNode', 'TNode', 'Length', 'Grid_Code' and 'Grid_Cod_1' were used. The 'ObjectID' is a unique number for every arc,

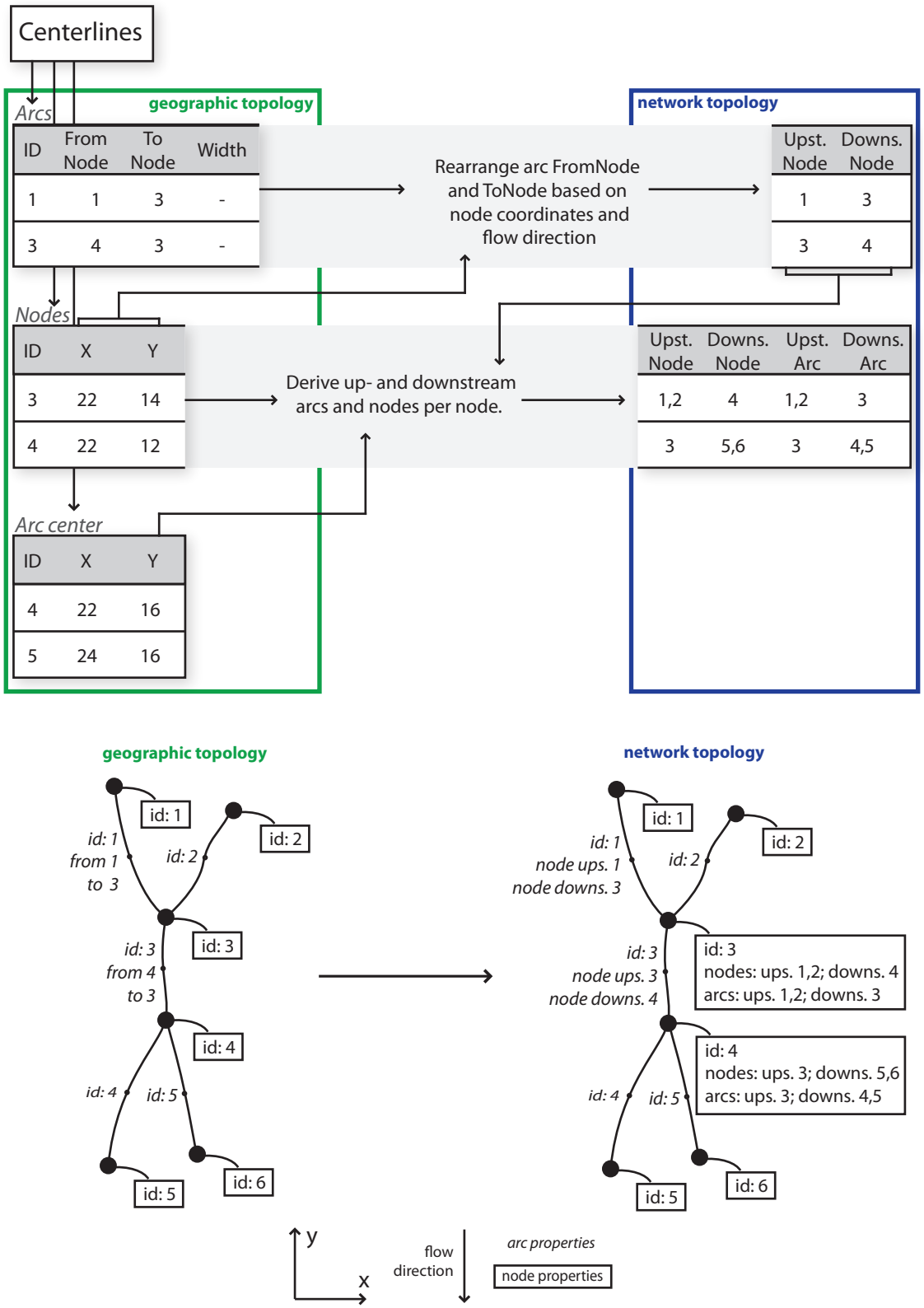

Figure 3.5 Flow chart of the transformation of a geographic topology to network topology (top diagram). The diagram on the bottom illustrates the difference in a geographic topology and a network topology.

'FNode' and 'TNode' contains the two nodes the arc is connected to, 'Length' contains the arc length. 'Grid_Code' and 'Grid_Cod_1' contains the mean and standard deviation of the channel width, respectively.

From the node attribute table (NAT) the fields 'ObjectID', 'X_Coord' and 'Y_Coord' were used. The field 'ObjectID' is a unique node numbers which related to the 'FNode' and 'TNode' field of the AAT, 'X_Coord' and 'Y_Coord' contain the coordinates of the node.

From the point attribute table (PAT) of the arc centre points the fields 'Orig_FID', 'Point_X' and 'Point_Y' were used. The field 'Orig_FID' relates the points to the 'ObjectID' of the arcs, 'Point_X' and 'Point_Y' contain the coordinates of the points.

A coordinate transformation (rotation and shift) was applied to the node and point coordinates to attain a coordinate system in the direction of the general flow direction:

$$\begin{bmatrix} i \\ j \end{bmatrix} = \begin{bmatrix} \cos(\theta) & -\sin(\theta) \\ \sin(\theta) & \cos(\theta) \end{bmatrix} \begin{bmatrix} x \\ y \end{bmatrix} + \begin{bmatrix} \Delta i \\ \Delta j \end{bmatrix} \tag{3.1}$$

where i and j are the new coordinates, j increases in flow direction and i is perpendicular to the flow direcion, x and y are the original coordinates, θ is the general flow direction, Δi and Δj are the shift in coordinates. The coordinate shift was applied to prevent the existence of negative coordinates.

Based on the downstream coordinate, j, the nodes connected to an arc, 'FNode' and 'TNode', were designated as upstream node or downstream node:

$$UN_a = \begin{cases} FN_a & if\ j(FN_a) < j(TN_a) \\ TN_a & if\ j(FN_a) > j(TN_a) \end{cases} \tag{3.2}$$

$$DN_a = \begin{cases} TN_a & if\ j(FN_a) < j(TN_a) \\ FN_a & if\ j(FN_a) > j(TN_a) \end{cases} \tag{3.3}$$

For every node the downstream arcs and nodes were queried: The arc-ids of all arc which had a certain node as upstream node were identified as that certain nodes downstream arcs. The node-ids of all downstream nodes of the downstream arcs were identified as the nodes downstream nodes. The same procedure was repeated for upstream arcs and nodes. The added arcs and nodes were sorted on i-coordinates, therefore channels on the left-hand side of another has a lower index. This is important when linking two networks that describe the same river at different moments (§3.4.1).

$$DA_n = UN_N == n \tag{3.4}$$

$$DN_n = DN(UN_N == n) \tag{3.5}$$

$$UA_n = DN_N == n \tag{3.6}$$

$$UN_n = UN(DN_N == n) \tag{3.7}$$

3.2.2 Additional node properties

Additional node properties were calculated which were used to differentiate between different types of nodes: confluences and bifurcations. Nodes with more than one downstream channel were identified as bifurcations, nodes with more than one upstream channel as confluence:

Table 3.1 Notation of various network elements and properties

Arc properties	Description	Coverage Field
WI_a	Width of *arc a*	`GRID_CODE`
LE_a	Length of *arc a*	`LENGTH`
TN_a	One of the two connected nodes to *arc a*	`TNODE`
FN_a	One of the two connected nodes to *arc a*	`FNODE`
DN_a	Downstream connected node to *arc a*	
UN_a	Downstream connected node to *arc a*	
$x(a)$	x-coordinate of *arc a* centre point	`POINT_X`
$y(a)$	y-coordinate of *arc a* centre point	`POINT_Y`
Node properties		
$x(n)$	x-coordinate of *node n*	`X_COORD`
$y(n)$	y-coordinate of *node n*	`Y_COORD`
$j(n)$	j-coordinate of *node n*	
$i(n)$	i-coordinate of *node n*	
DA_n	Downstream connected arcs of *node n*	
DN_n	Downstream connected nodes of *node n*	
UA_n	Upstream connected arcs of *node n*	
UN_n	Upstream connected nodes of *node n*	
DNA_n	Angles to downstream connected nodes of *node n*	
UNA_n	Angles to upstream connected nodes of *node n*	
BI_n	Equals 1 when *node n* is a bifurcation, 0 otherwise	
CO_n	Equals 1 when *node n* is a confluence, 0 otherwise	
Network		
k_n	Degree of *node n*, number of connected edges	
k_n^{in}, k_n^{out}	In-degree and out-degree, number of upstream and downstream connected edges	
M^x	Connectivity matrix with x as weights	
$M_{n,m}$	Entry in the connectivity matrix between *node n* and m, $M_{n,m} \neq 0$ when *node n* is connected to m	

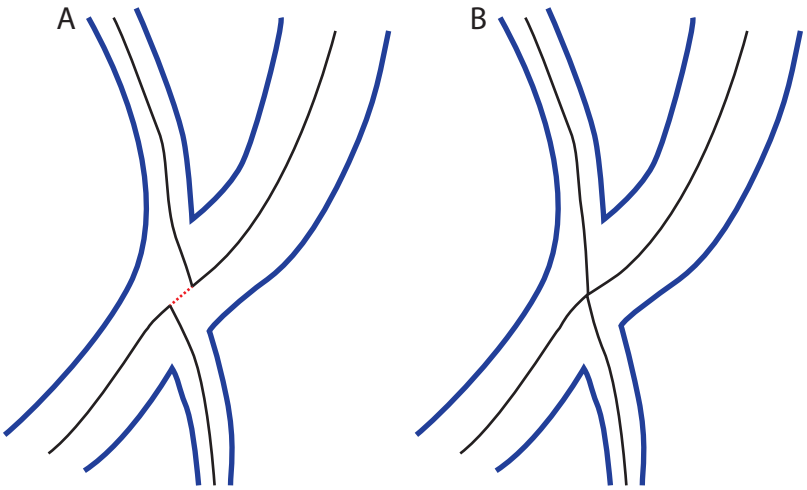

Figure 3.6 Illustration of a small element (much shorter than its length) which were removed from the dataset. Blue lines are bank lines, black lines are centrelines and the red-dotted line is the small element to be removed. Such elements were often present at a complex junction at a bifurcation-confluence unit. The removal includes the adjustment of the dataset for all directly connected arcs and nodes. The resulting node is identified as both a bifurcation as a confluence.

$$BI_n = \begin{cases} 1 & if\ \#DA_n > 1 \\ 0 & else \end{cases} \tag{3.8}$$

$$CO_n = \begin{cases} 1 & if\ \#UA_n > 1 \\ 0 & else \end{cases} \tag{3.9}$$

The angle to downstream and upstream nodes were calculated, this was used for matching nodes between two networks of the same system at different dates (§3.4.1).

$$DNA_{n,m} = \arctan\left(\frac{x(n)-x(m)}{y(n)-y(m)}\right) \mid m \in DN_n \tag{3.10}$$

$$UNA_{n,m} = \arctan\left(\frac{x(n)-x(m)}{y(n)-y(m)}\right) \mid m \in UN_n \tag{3.11}$$

3.2.3 Enhancing the channel network

Unwanted network elements were removed before building a connectivity matrix. Small channel segments exist in the dataset which often have no physical meaning (Fig. 3.6), these small elements interfere with the analysis of the network. Such small elements existed in complex junction of more than three channels. The river network was in such cases often built of two or more simple nodes with three connected channels, which were in turn connected via a small channel segment. A better description of such complex junctions would be that all channels are connected in one node. To remove these elements, all nodes which were wider than twice their length were removed from the dataset. Connectivity properties of connected nodes were adapted to the new situation.

3.2.4 Building the network connectivity matrix

From the network topology connectivity matrices were built. This matrix allows the calculation of various network measures (§3.3). An entry $M_{n,m} = w$ in the matrix denotes a connection from node n to node m with weight w. If the network is unweighed, $w = 1$. Two arc properties are available to use as weight: length and width. Depending on the used analysis, different weights can be used. Various weights were used: width, length, width divided by length and the inverse of width and length, resulting in five connectivity matrices per network:

$$M^{wi}_{n,m} = WI_a \mid m = DN_n, a = DA_n \tag{3.12}$$
$$M^{wi^{-1}}_{n,m} = WI_a^{-1} \mid m = DN_n, a = DA_n \tag{3.13}$$
$$M^{le}_{n,m} = LE_a \mid m = DN_n, a = DA_n \tag{3.14}$$
$$M^{le^{-1}}_{n,m} = LE_a^{-1} \mid m = DN_n, a = DA_n \tag{3.15}$$
$$M^{wi \cdot le^{-1}}_{n,m} = WI_a \cdot LE_a^{-1} \mid m = DN_n, a = DA_n \tag{3.16}$$

3.3 River network analysis

The connectivity matrices for every channel network were used as input in the Brain Connectivity Toolbox (BCT) by *Rubinov and Sporns* (2009). With this toolbox, various network measures were calculated. These measures are calculated per node. The network measures were written to a table per network, which was linked to the GIS dataset of the network for visualisation. Measures were calculated using the four different weights described in the previous section. Interpretation of different combinations of weights and measures are described in Chapter 4.

For all weights described in Eqs. 3.12 to 3.16 and for an unweighed variant of the networks, the clustering coefficient, the betweenness and the modularity were calculated. A correction was applied to the betweenness and this measure was applied to arcs, as described in the following sections.

3.3.1 Normalised betweenness

The betweenness centrality is highly affected by the boundaries of the river network. Since the river network has a start and an end, the betweenness is zero at both the most upstream and downstream node. The betweenness reaches a maximum in the middle of the used network. This signal dominates the betweenness. This effect is not present in closed networks like social networks for which this method is developed.

The betweenness was corrected by normalising the values to the potential betweenness per node. The betweenness is defined as the fraction of shortest paths in the network which pass through a node. The potential maximum number of shortest paths though a node in a directed network, like a river network, is the number of nodes upstream of that nodes multiplied by the number of nodes downstream of that node.

$$Bc_n^{norm} = \frac{Bc_n}{|j(N) < j(n)| \cdot |j(N) > j(n)|} \tag{3.17}$$

3.3.2 Betweenness per arc

Network measures are calculated per node. The betweenness is also relevant for arcs, as this is usefull for visualisation and used in the calculation of the weighted braiding index. The betweenness was calculated for every arc in the network, in addition to the betweenness per node as calculated using the BCT. The number of connections through an arc is the lowest value of connections through both nodes the arc connects to. The betweenness per arc was calculated by taking the lowest value of either the up- or downstream node:

$$Bc_a^{norm} = min\left(Bc_n^{norm}(UN_a), Bc_n^{norm}(DN_a)\right) \tag{3.18}$$

3.3.3 Braiding index

The braiding index (B.I.) for every river channel network was calculated as a variable along the river and as a single value for the whole network. The network topology table was used to determine the change in number of channels per node (number of connected upstream channels minus the number of connected downstream channels). The number of parallel channels was calculated at every node by walking through all nodes from upstream to downstream and using the change in number of channels. The BI values were assigned per node and represent the number of parallel channels downstream of that node.

$$sort\ n : j(n) < j(n+1) \tag{3.19}$$

$$BIX(n) = BIX(n-1) - k_n^{in} + k_n^{out} \tag{3.20}$$

The average braiding index was calculated by dividing the weighted (Riemann) sum of $BIX(n)$ by the total length of the part of the river under consideration. The weight for the Riemann sum is the distance which the corresponding BI represents, the distance to the next node in downstream direction:

$$BIX_N = \left(\sum_{n \in N} BIX(n)\left(j(n) - j(n-1)\right)\right)\left(max(j) - min(j)\right)^{-1} \tag{3.21}$$

3.4 Bifurcation development

In order to analyse the development of individual elements in the river channel network, the elements between two networks at different dates needs to be linked. The changes in properties of the elements are then used to identify changes. In this section the procedure to link nodes between two networks at different dates is described and the calculation of bifurcation asymmetry and the method to analyse the bifurcation asymmetry development are described.

3.4.1 Linking nodes

A bifurcation or confluence which is present at two dates, is present in both river channel network of those dates. These two nodes are likely to show a lot of resemblance, but are not identical. The following procedure was used to find nodes in two river channel networks which are most likely to be the same:

1. Bifurcations were only linked to bifurcations ($BI_n = 1$) and confluences ($CO_n = 1$) were only linked to confluences.

2. Only nodes with three connected channels ($k_n = 3$) were used. Which are bifurcations with two downstream channels ($k_n^{out} = 2$) and confluences with two upstream channels ($k_n^{in} = 2$).

3. A score was calculated for all possible combinations of nodes between both networks. The score is defined as the product between the distance in node location and the root mean square of the change in angle to connected nodes, nodes with more resemblance have lower scores:

$$\begin{aligned} S_{t1,t2} &= \sqrt{(x(t_1) - x(t_2))^2 + (y(t_1) - y(t_2))^2} \ldots \\ &\quad \sqrt{\frac{(DNA_{t1,1} - DNA_{t2,1})^2 + (DNA_{t1,2} - DNA_{t2,2})^2}{2}} \end{aligned} \tag{3.22}$$

   where $DNA_{n,m}$ is the angle from node n to the m-th downstream connected node. DNA is used for bifurcation, UNA is used for confluences. Only simple (3 connected channels) bifurcations and confluences were used for linking nodes, thus only $m = 2$ exist.

4. For every node in the first channel network, all nodes in the second image within a specified range were selected as possible candidates. The width of the widest channel connected to the node in the first channel network was used as search range.

5. For all candidates, if any, the candidate with the lowest score to the node under consideration was selected.

6. If more than one node linked to the same node, only the node with the highest score was retained. If the removed nodes had other candidates, those were considered again. These steps were repeated until there were no nodes present which had been linked to from multiple nodes.

3.4.2 Bifurcation asymmetry

The degree of unbalance of a bifurcation can be addressed by the asymmetry of discharge in the two downstream channels. The discharge asymmetry is defined as follows:

$$\Delta Q = \frac{Q_b - Q_c}{Q_a} \tag{3.23}$$

where Q_b and Q_c are the discharges in the two downstream channels and Q_a is the discharge in the upstream channel. ΔQ is equal to zero when the discharge is evenly distributed and equal to 1 or -1 when the the water only flows in one of the branches, thus one of the two is closed (*Bertoldi et al.*, 2009b).

Discharge of individual channels is not known and cannot be estimated from satellite images since the channel depth and flow velocity are unknown. The asymmetry can only be calculated from the difference in channel width. Based on Eq. 3.23, the following equation was used to calculate the bifurcation asymmetry from a channel network:

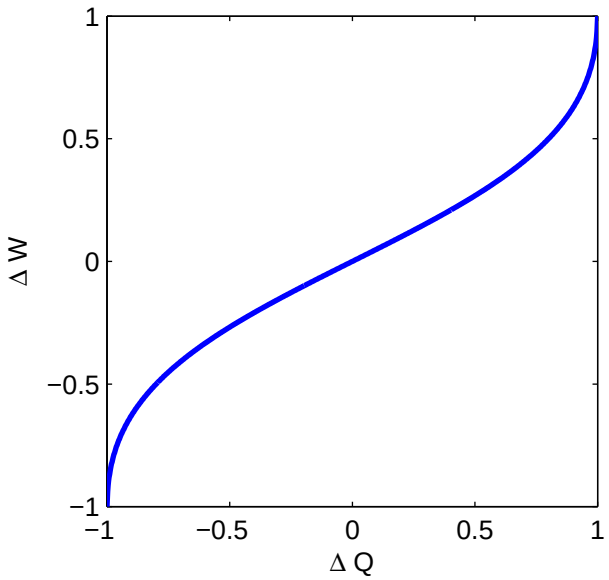

Figure 3.7 Relation between bifurcation asymmetry based on discharge and based on channel width. A width discharge relation of $W \sim Q^{0.5}$ is assumed.

$$\Delta W = \frac{W_b - W_c}{W_b + W_c} \tag{3.24}$$

where ΔW is the asymmetry, W_b and W_c are the widths of the downstream channels. Eq. 3.24 is formulated such that ΔW does not exceed 1 or -1. These values correspond with a closure of one of the two channels. The theoretical relation between ΔQ and ΔW is not linear, but key values of 0, 1 and -1 correspond (Fig. 3.7).

3.4.3 Bifurcation asymmetry development

To analyse the development of bifurcation asymmetry, the bifurcation asymmetry of all linked nodes at one moment ($t = 1$) were plotted against the bifurcation asymmetry at a later date ($t = 2$). This results in a plot with distinct areas which have different interpretation (Fig. 3.8).

3.5 Weighted braiding index

The braiding index of a river is a measure for the number of parallel channels of a river. To obtain a more accurate measure for the actual braiding index, only the active channels should be used, this results in the Active Braiding Index (*Egozi and Ashmore*, 2008). Either way, the braiding index is still biased by small channels. For example: a river with three parallel channels with equal discharge has the same braiding index as a river with three parallel channels of which one carries 98 percent of the discharge and the other two both 1 percent of the discharge.

The weighted braiding index (wBI) is obtained by taking the importance of the channel into account. A cross section with one dominant channel and many small channels has a lower wBI than a cross section where the discharge is spread more evenly across the channels. The betweenness centrality was used as measure for importance of a chan-

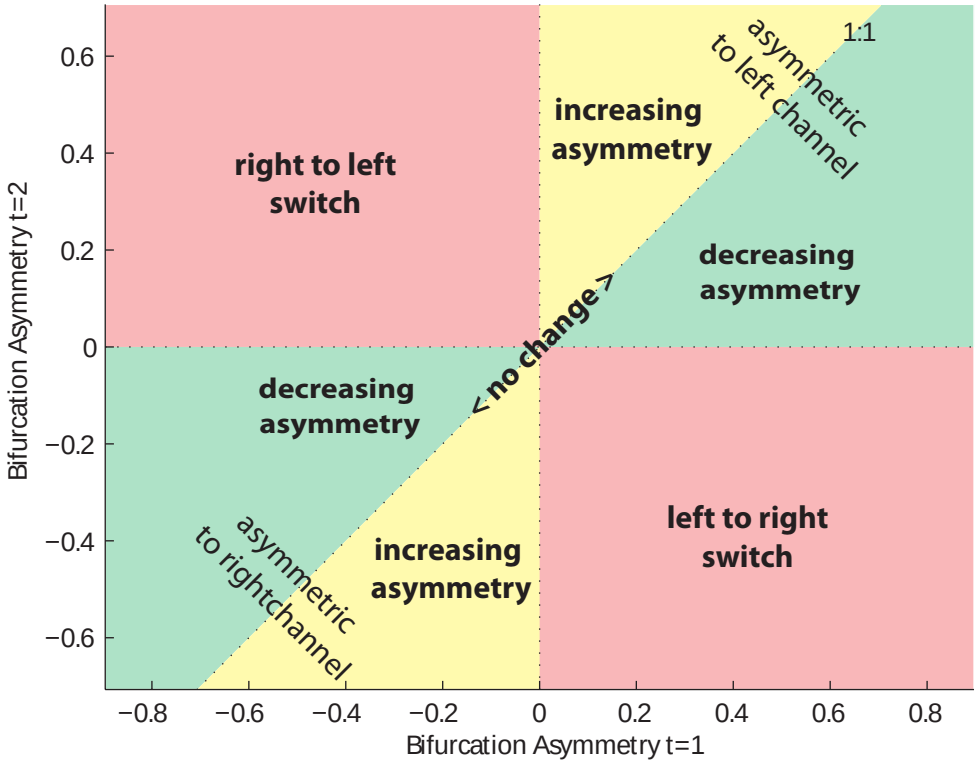

Figure 3.8 Interpretation of bifurcation asymmetry development plot. Bifurcations which plot in the yellow and green quadrants are bifurcations with remain asymmetrical to the same direction, bifurcations with a larger left channel plot in the upper right quadrant, bifurcations with a larger right channel plot in the lower left quadrant. When the bifurcation asymmetry increases, the bifurcations plot in the yellow areas, when it decreases in the green areas. When the asymmetry switches from left to right or vice versa, the bifurcations plot in the red quadrants.

nel. The theoretical betweenness per channel when the discharge is spread equally is the sum of the betweenness values in a cross section divided by the number of channels. This value was compared to the betweenness per channel. Every channel with a betweenness value higher than half the betweenness value when evenly distributed were counted as a channel for the wBI. The same procedure was used as described for the braiding index (Eqs. 3.19–3.21).

4 Results and interpretation

In this chapter, the results are presented and interpreted. Possible meaningful interpretations in terms of river dynamics are given to network measures in the first section. In the second section, the results of morphological measures are presented.

4.1 Interpretation of network measures

In this section meaningful morphological explanations of network measures are described. From various network measures available, a few may contain relevant information for river network analysis. These are the betweenness centrality (important elements), clustering coefficient (identification of braiding clusters) and the modularity (separation of different sub-network modules). Whether these measures are useful, is described here.

4.1.1 Betweenness centrality

The betweenness centrality is defined as the fraction of shortest paths between all nodes in the network that pass though a given element in the network and can be interpreted as a measure of importance of an element in the network. Elements with a higher betweenness centrality influence a larger part of the network than elements with a lower betweenness centrality. This measure is often used in studies of social networks to identify the importance of relations between persons (*Freeman*, 1987). This measure gives more information than just the number of connections as the structure of the whole network influences the betweenness centrality.

In a river channel network, the betweenness centrality gives information about the most important bifurcations, confluences and channels (Fig. 4.1). The betweenness centrality contains more information than just the channel width, length or discharge, the whole network structure is used and properties of both up and downstream elements are taken into account (Fig. 4.2). This corresponds with the propagation of changes in a river as changes in a river propagate in both up- and downstream direction. Due to the backwater effect a perturbation or change in the river has an effect on the water stage in upstream direction. A change in discharge (or discharge distribution at a bifurcation) has an effect on the discharge in all channels downstream of the change.

Choice of weight

The calculation of betweenness centrality can involve a weight. This weight, together with the flow direction, is used for the calculation of path lengths between nodes. There are two properties available in the dataset to use as weight: channel length and width. Both have

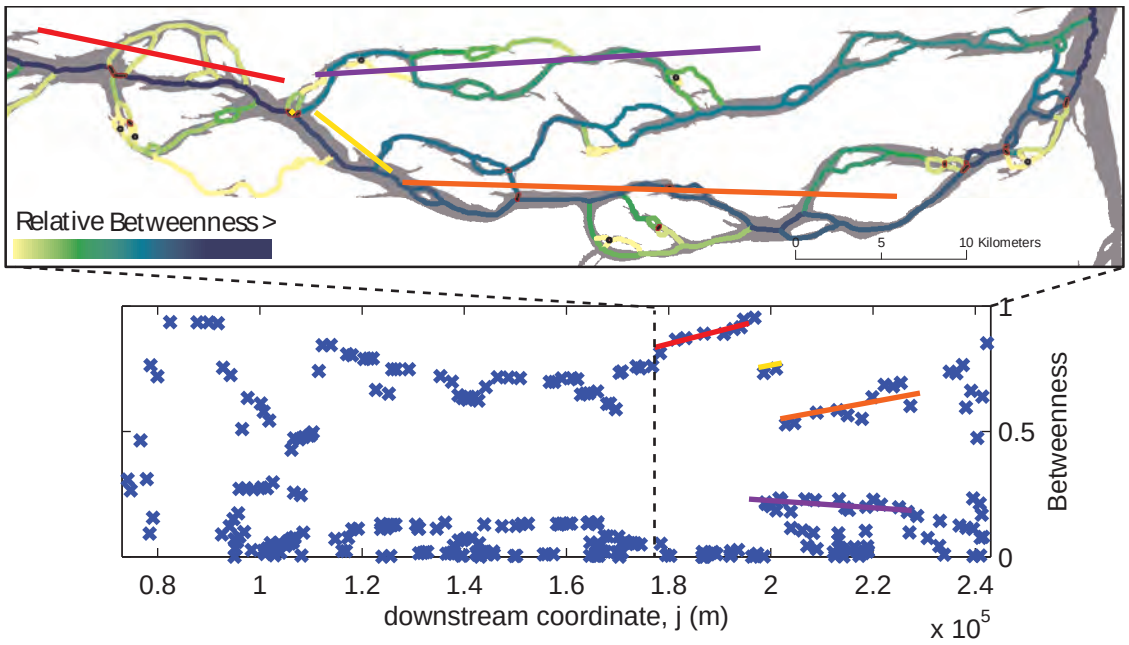

Figure 4.1 Demonstration of the use of betweenness centrality (BC) as measure for importance of channel segments. length/width is used as weight. The upper image is a map of a part of the whole river network. In the bottom image the BC of al nodes, plotted in downstream direction are shown. Three main channels are highlighted in both images. The sudden decrease of BC is the result of a bifurcation into two branches with a high BC.

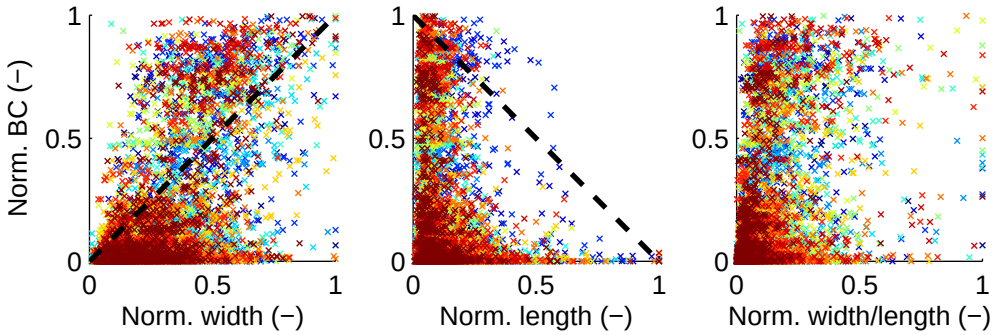

Figure 4.2 Relation between channel width and channel length and betweenness centrality for every element in the network. In general, channels with a higher width or shorter length result in a higher BC. All deviations from this relation are the result of the network structure. There is no direct relation between the used weight (length/width) and the BC per element, indicating that the largest part of the BC results from values of other elements in the network. Values are normalised to allow comparison between multiple channel networks (every network has a different colour). There are no differences in trends between different networks.

a physical justification to be used as weight and the combination of the two gives the best result, as explained in the following paragraphs (also see Fig. 4.2).

When the length of an arc between two nodes is used, the importance of a node is defined based on the actual shortest distances. In a river, a shorter channel has a gradient advantage over a longer channel. Water is more likely to flow through a shorter channel than a longer channel covering the same elevation difference.

The inverse of the width of a channel can be interpreted as a resistance. Assumed that wider channels transport more water, wider channels are more important in terms of discharge. At a bifurcation, more water will flow through the larger channel and this channel should be identified as more important. In terms of virtual path length (as this is used in network analysis), wider channels are closer to each other in term of paths of least resistance. This can be expressed by using the inverse of the width as path length.

The combination of these two weights can be combined: length divided by width. This is the most convenient weight to address the importance of network elements in the calculation of betweenness centrality.

4.1.2 Clustering coefficient

The clustering coefficient is a measure for the interconnectedness of a node's neigbour nodes. A braided river has many bifurcations and confluences close to each other. Nodes in braided reaches are likely to have a high clustering coefficient. The rate of braiding can be pointed out even more if the inverse of the distance between two nodes is used as weight for the connection: nodes closer together get a higher weight and thus a higher clustering coefficient.

A major drawback of the clustering coefficient is that it only uses the direct neighbours of a node. Furthermore, two connections from a node to the same node do not increase the clustering coefficient. Nodes with high interconnectedness are identified with this method (Fig 4.3). A cluster of channels in a braided river also include two channels from the same bifurcation to the same confluence and clusters spanning further that the direct neighbours. Therefore, the clustering coefficient can not be used for consistent identification of braided reaches in a river network.

4.1.3 Modularity

The concept of the modularity is to extract individual groups of nodes from a network which have a high interconnectedness. In terms of river morphological terms, these could be parts of the river which have different properties like a higher degree of braiding or a distinct branch.

The extraction of a modular structure is not satisfactory due to the limited range of degree of nodes, most nodes have 3 connections which is also the minimum in the river networks used. Distinct modules are recognised, but modules reach over multiple branches and / or consist of only a part of a branch (Fig. 4.4). Extraction of a modular structure is useful when distinction is needed between sub-networks which are more complex than the overall network structure. The relative simple network of a river (a limited range of node degrees) does not allow a successful distinction of modules.

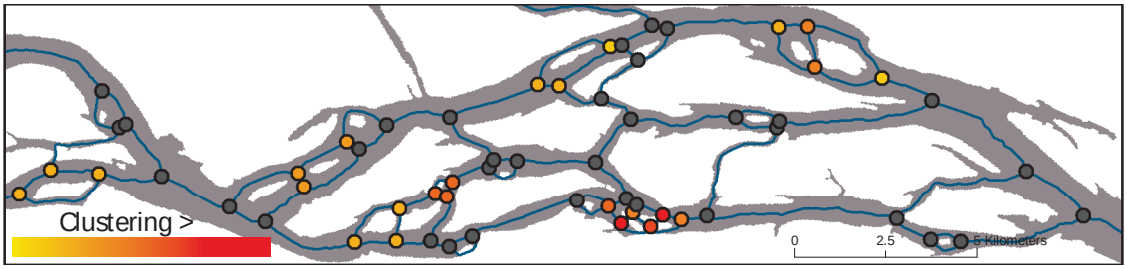

Figure 4.3 Demonstration of the use of clustering coefficient as measure for braided reaches. Triangles of channels are identified in this map, with higher values for more compact clusters. However, when two nodes are connected to each other with two channels, no cluster is identified while this is interpreted as braiding. Also, when there is a quadrilateral of channels, this is also not identified as a cluster. Note: black nodes have a clustering coefficient of 0.

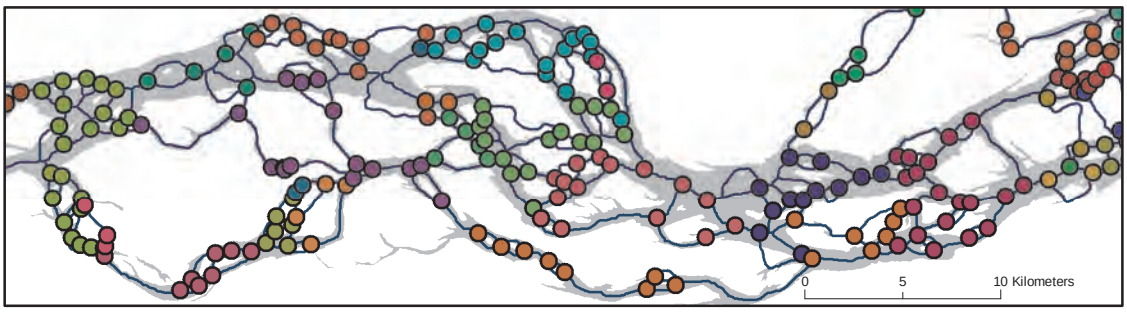

Figure 4.4 Demonstration of the use of modularity. Every colour represents a different module. Distinct clusters of nodes are identified, but these clusters do not correspond with morphological features. For example, the green module on the left hand side consist of a part of the smaller channel on the bottom but also consist of (a part of) the broad complex braided reach at the top. In this figure, length / width is used as weight, all other weights produce even more inconsistent results.

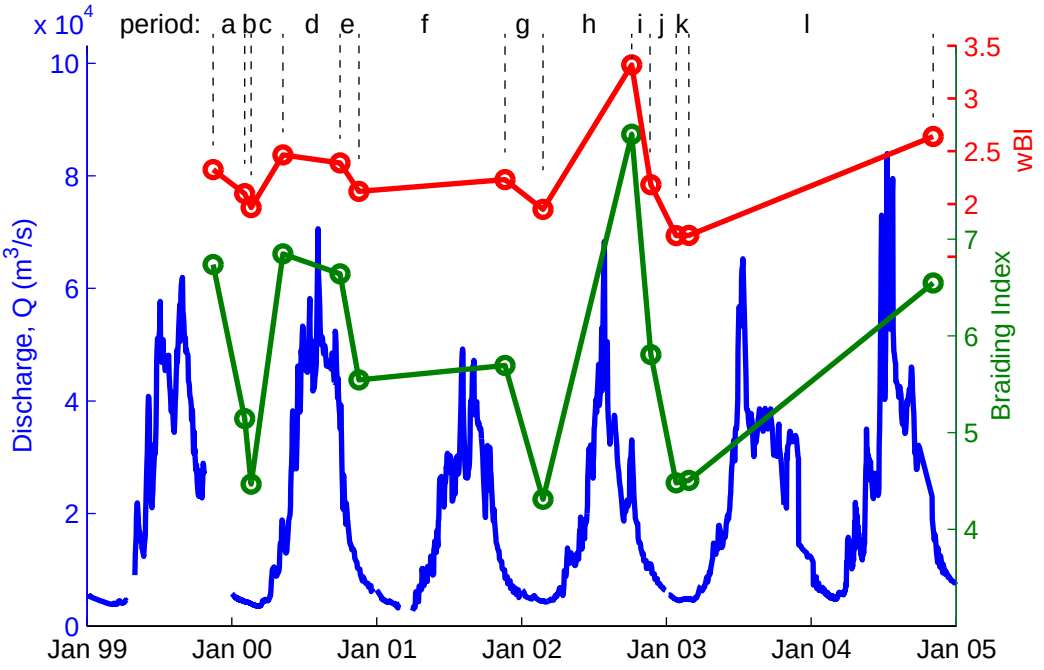

Figure 4.5 Hydrograph, braiding index (BI) and weighted braiding index (WBI) 1999 - 2004. The BI fluctuates between 4 and 7. It shows a decrease during periods of low discharge and an increase during a period of high discharge. The WBI fluctuates between 1.9 and 2.4, the main signal is similar to the BI. The lowest values of WBI are lower than 2, both are February scenes at the end of the dry season. The periods a-l correspond with the subfigures of Fig. 4.6.

4.2 River network evolution

In this section, the results of the river network analysis are presented. Morphology related measures are presented in contrast to the previous section where network related measures were presented. First, the development of braidingness and the relation to the development of individual bifurcations are presented. Secondly, the development of a dominant channel is analysed. The latter is done by analysing the development of individual bifurcations and the weighted braiding index, which combines the braiding index with a measure of channel importance, the betweenness centrality, derived from the river network.

4.2.1 Braiding index

For every extracted river network, the overall braiding index was determined. Two relations are visible when comparing the braiding index to the discharge regime: 1) the braiding index increases during periods of high discharge and 2) the braiding index decreased in periods of low discharge (Fig. 4.5, Tab.4.1). The braiding index rises op to six or higher almost every year there is a scene present at the end of the summer. The lowest braiding indices are found in the dry season in the winter, the braiding index drops to about 4.5 every year (Tab. 4.3). The braiding index shows less variation when only scenes of the same season (inter- and intra-annual) are considered (Tab. 4.2, 4.3).

Table 4.1 Dataset properties and changes for all consecutive dates. Letters a-l correspond with the periods in Fig. 4.5 and 4.6.

date	19991115	$a \rightarrow$	20000203	$b \rightarrow$	20000219	$c \rightarrow$	20000509	$d \rightarrow$	20000930
BI	6,7	- 1,6	5,1	- 0,7	4,5	+ 2,4	6,8	- 0,2	6,6
wBI	2,3	- 0,2	2,1	- 0,1	2,0	+ 0,5	2,5	- 0,1	2,4
nodes	581	- 295	286	+ 2	288	+ 255	543	- 95	448
bifurc.	277	- 140	137	+ 4	141	+ 114	255	- 50	205
confl.	299	- 161	138	+ 5	143	+ 137	280	- 52	228
linked bi.		85		96		58		86	
linked co.		92		100		57		102	

date	20000930	$e \rightarrow$	20001117	$f \rightarrow$	20011120	$g \rightarrow$	20020224	$h \rightarrow$	20021006
BI	6,6	- 1,1	5,5	+ 0,1	5,7	- 1,4	4,3	+ 3,8	8,1
wBI	2,4	- 0,3	2,1	+ 0,1	2,2	- 0,3	1,9	+ 1,4	3,3
nodes	448	+ 12	460	+ 42	502	- 165	337	+ 184	521
bifurc.	205	+ 12	217	+ 15	232	- 76	156	+ 75	231
confl.	228	+ 6	234	+ 26	260	- 90	170	+ 107	277
linked bi.		66		87		86		17	
linked co.		77		106		113		22	

date	20021006	$i \rightarrow$	20021123	$j \rightarrow$	20030126	$k \rightarrow$	20030227	$l \rightarrow$	20041104
BI	8,1	- 2,3	5,8	- 1,3	4,5	+ 0,0	4,5	+ 2,0	6,5
wBI	3,3	- 1,1	2,2	- 0,5	1,7	+ 0,0	1,7	+ 0,9	2,6
nodes	521	- 33	488	- 139	349	- 42	307	+ 219	526
bifurc.	231	- 11	220	- 62	158	- 17	141	+ 95	236
confl.	277	- 21	256	- 79	177	- 19	158	+ 121	279
linked bi.		68		84		111		37	
linked co.		80		101		123		61	

Table 4.2 Dataset properties and changes for all autumn scenes.

date	19991115	$\rightarrow$	20001117	$\rightarrow$	20011120	$\rightarrow$	20021123	$\rightarrow$	20041104
BI	6,7	- 1,2	5,5	+ 0,1	5,7	+ 0,1	5,8	+ 0,7	6,5
wBI	2,3	- 0,2	2,1	+ 0,1	2,2	- 0,0	2,2	+ 0,5	2,6
nodes	581	- 121	460	+ 42	502	- 14	488	+ 38	526
bifurc.	277	- 60	217	+ 15	232	- 12	220	+ 16	236
confl.	299	- 65	234	+ 26	260	- 4	256	+ 23	279
linked bi.		93		87		86		73	
linked co.		113		106		113		93	

Table 4.3 Dataset properties and changes for all winter scenes.

date	20000203	$\rightarrow$	20000219	$\rightarrow$	20020224	$\rightarrow$	20030126	$\rightarrow$	20030227
BI	5,1	- 0,7	4,5	- 0,2	4,3	+ 0,2	4,5	+ 0,0	4,5
wBI	2,1	- 0,1	2,0	- 0,0	1,9	- 0,2	1,7	+ 0,0	1,7
nodes	286	+ 2	288	+ 49	337	+ 12	349	- 42	307
bifurc.	137	+ 4	141	+ 15	156	+ 2	158	- 17	141
confl.	138	+ 5	143	+ 27	170	+ 7	177	- 19	158
linked bi.		96		36		46		111	
linked co.		100		51		58		12	

4.2.2 Bifurcation asymmetry development

For the individual periods between all consecutive scenes, the bifurcation asymmetry development of individual, linked, bifurcations were determined (Fig. 4.6). There are two periods where both river networks fall in the same season and have a comparable discharge: period b (20000203 – 20000219) and period k (20030126 – 20030227). In period b, most of the bifurcations show a slight increase in bifurcation asymmetry, in period k the bifurcation asymmetry is more or less equal in both scenes (Fig. 4.6b,k). An important observation for period k, is that the (weighed) braiding index is already very low at the start of the period, the lowest observed in the studied period – in other words, there is not much space left for further increase of bifurcation asymmetry as there was already a strong dominant channel present.

In the other periods, there is a discharge difference or a flood peak present between the dates of the river channel networks. Both effects change the river channel pattern, which either causes a change in bifurcation asymmetry or frustrates the linking of bifurcations between the two networks. Hence, the bifurcation asymmetry plots are rather chaotic. Periods with a high difference in braided index or weighted braiding index, for example periods h and i, show the most chaotic development of bifurcation asymmetry (Tab. 4.1). Whether this is due to a change in bifurcation asymmetry or due to linkage errors is unclear, nevertheless both discharge differences as floods cause the channel pattern to change.

Bifurcation asymmetry trends are not observed in intra-annual linked scenes in the same season, due the large difference in channel and bifurcation location and configuration (Appendix B). Too much morphological development frustrates the bifurcation linking process in these cases.

4.2.3 Dominant channel formation / weighted braiding index

An increase of bifurcation asymmetry will lead to the development of a dominant channel. When a bifurcation is still present, but becomes more asymmetrical, the amount of channels will remain the same, thus the braiding index will not change. In order to assess whether a dominant channel is formed, the relative importance of river channel segment is used. The importance of a channel is addressed by the betweenness centrality calculated from the channel network. This is the basis of the weighted braiding index, which is a measure for number of important channels per cross section. The weighted braiding index shows some correlation with the braiding index, but deviations are present (Fig. 4.7).

The development of bifurcation asymmetry correspond with changes in wBI. For example, the increase of bifurcation asymmetry in period b (20000203 – 20000219) described in the previous section corresponds with a decrease of weighted braiding index (2.1 to 2.0). In period k (20030126 – 20030227), where the bifurcation asymmetry is more or less equal in both scenes, the wBI (1.7) and BI (4.5) are equal (Fig. 4.5, Tab. 4.1).

As pointed out in the previous section, it has not been successful to assess the development of bifurcation asymmetry in all periods due to the large changes caused by discharge peaks and long temporal distances between scenes. The wBI together with the BI can be used as an indirect measurement of bifurcation development: an increase of bifurcation development (decrease of wBI, equal BI) or reactivation of channels (increase of wBI, equal BI), avulsion (increase or equal wBI, increase of BI) and channel closures

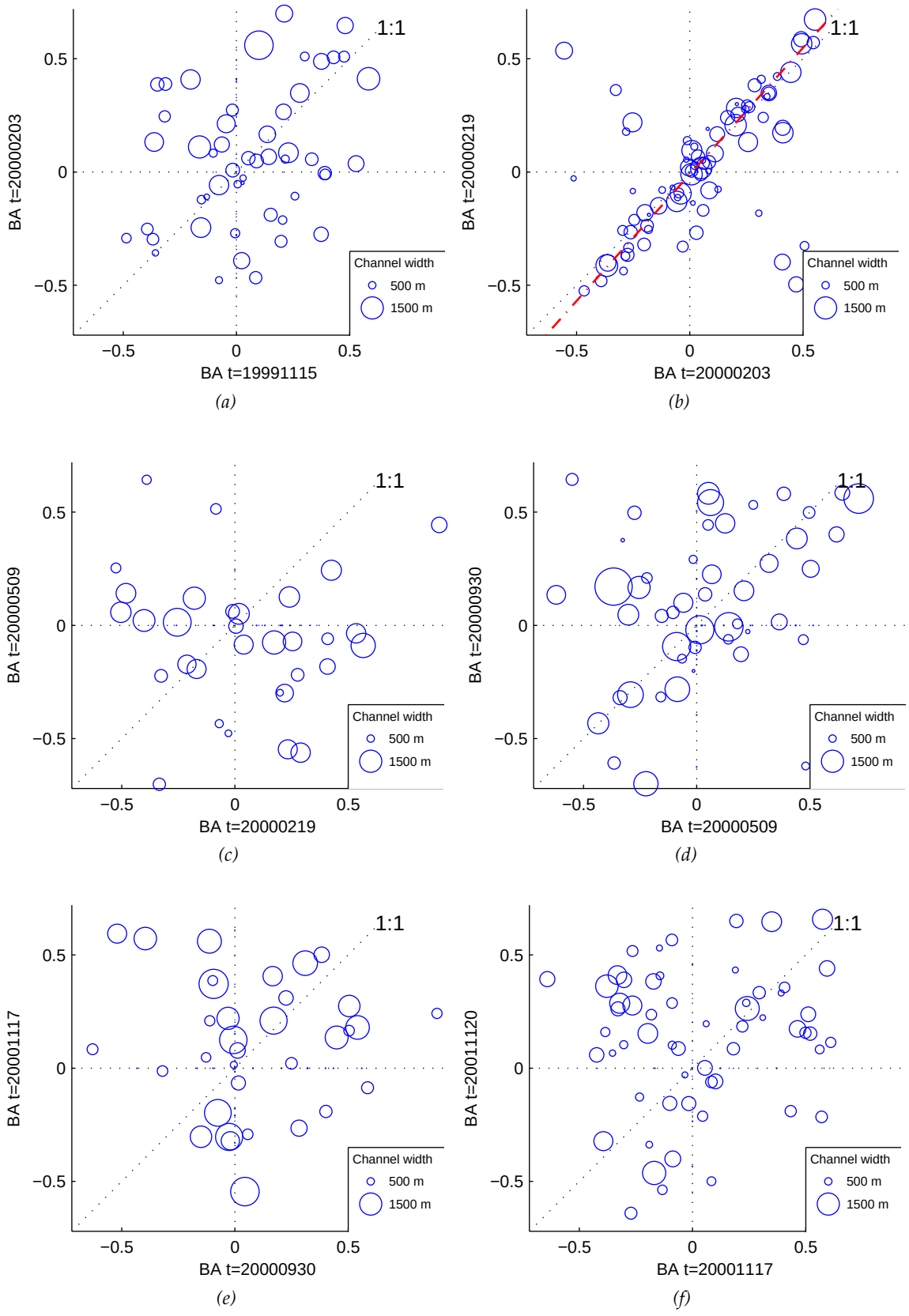

Figure 4.6 Bifurcation asymmetry development for all succeeding scenes. See Fig. 3.8 for interpretation of plots. Circle radius represent the mean channel width of both downstream channels. The red line shows a weighted linear regression as guide, if convenient. (Continued on page 45)

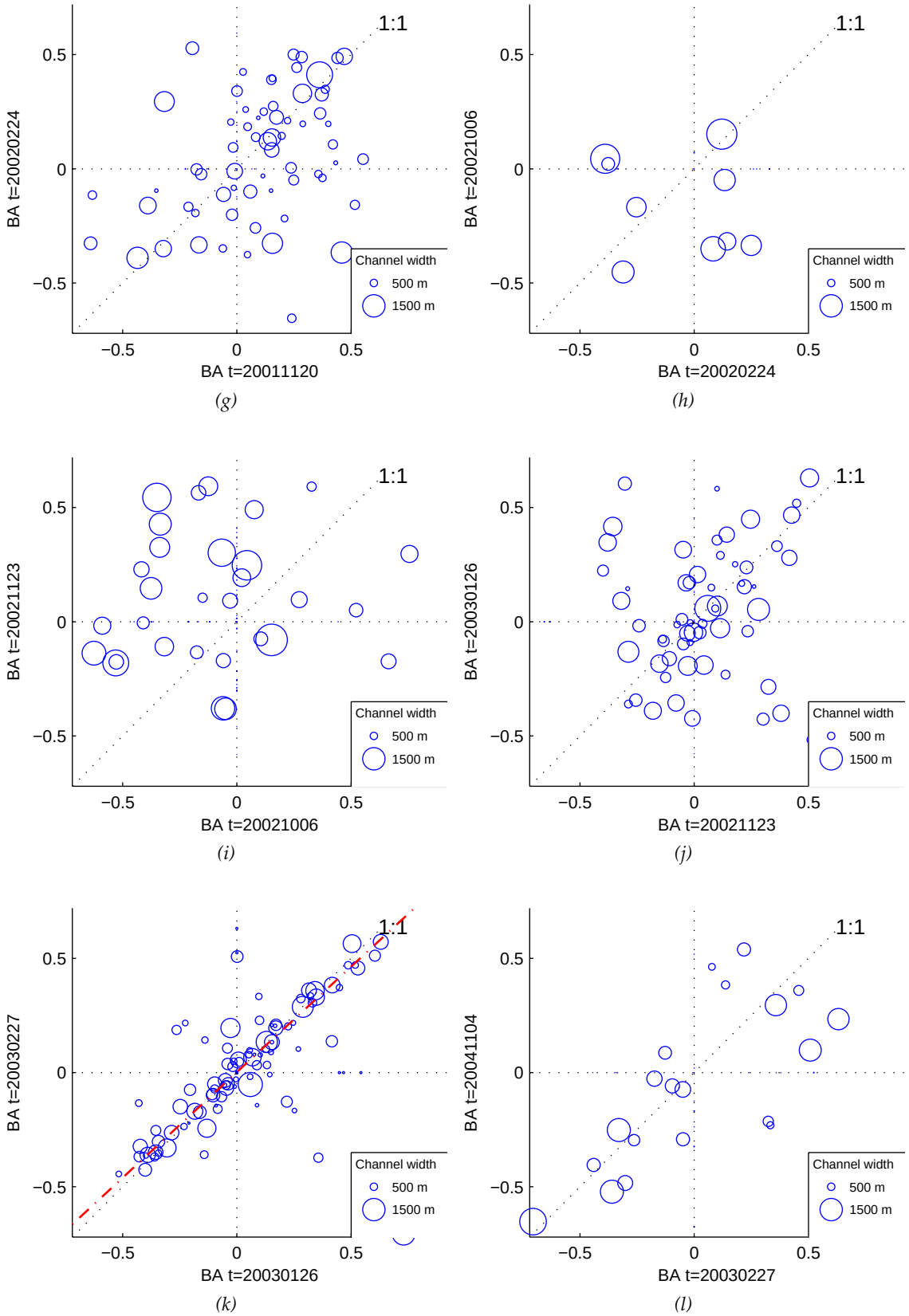

Figure 4.6 (Continued from page 44) Bifurcation asymmetry development for all succeeding scenes. See Fig. 3.8 for interpretation of plots. Circle radius represent the mean channel width of both downstream channels. The red line shows a weighted linear regression as guide, if convenient.

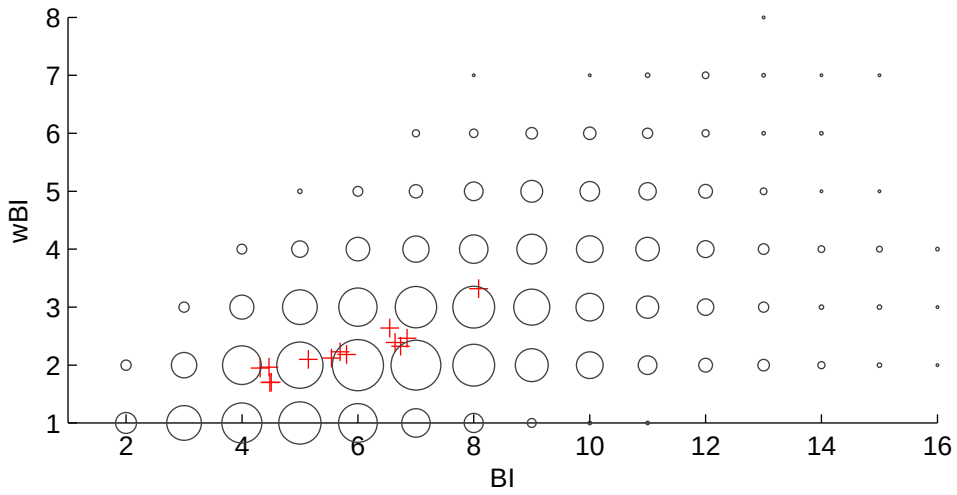

Figure 4.7 Braiding index (BI) vs weighted braiding index (wBI) for all individual cross-sections (circles, size represents occurrences of specific BI-wBI combination) and mean per scene (red '+').

(decrease or equal wBI and decrease of BI) can be derived from these measures.

An important observation of the weighted braiding index in the used river networks is that values of one are often present in some parts of the river, these are absent in the braiding index for the current datasets (for example Fig. 4.8, all Figures of this kind in Appendix C). Values of one indicate cross-sections with one dominant channel with a high importance and thus no active braiding. The overall wBI does not get this low, but values below 2 are present during the dry season (Fig. 4.5), indicating that there is hardly any active braiding going on in these periods.

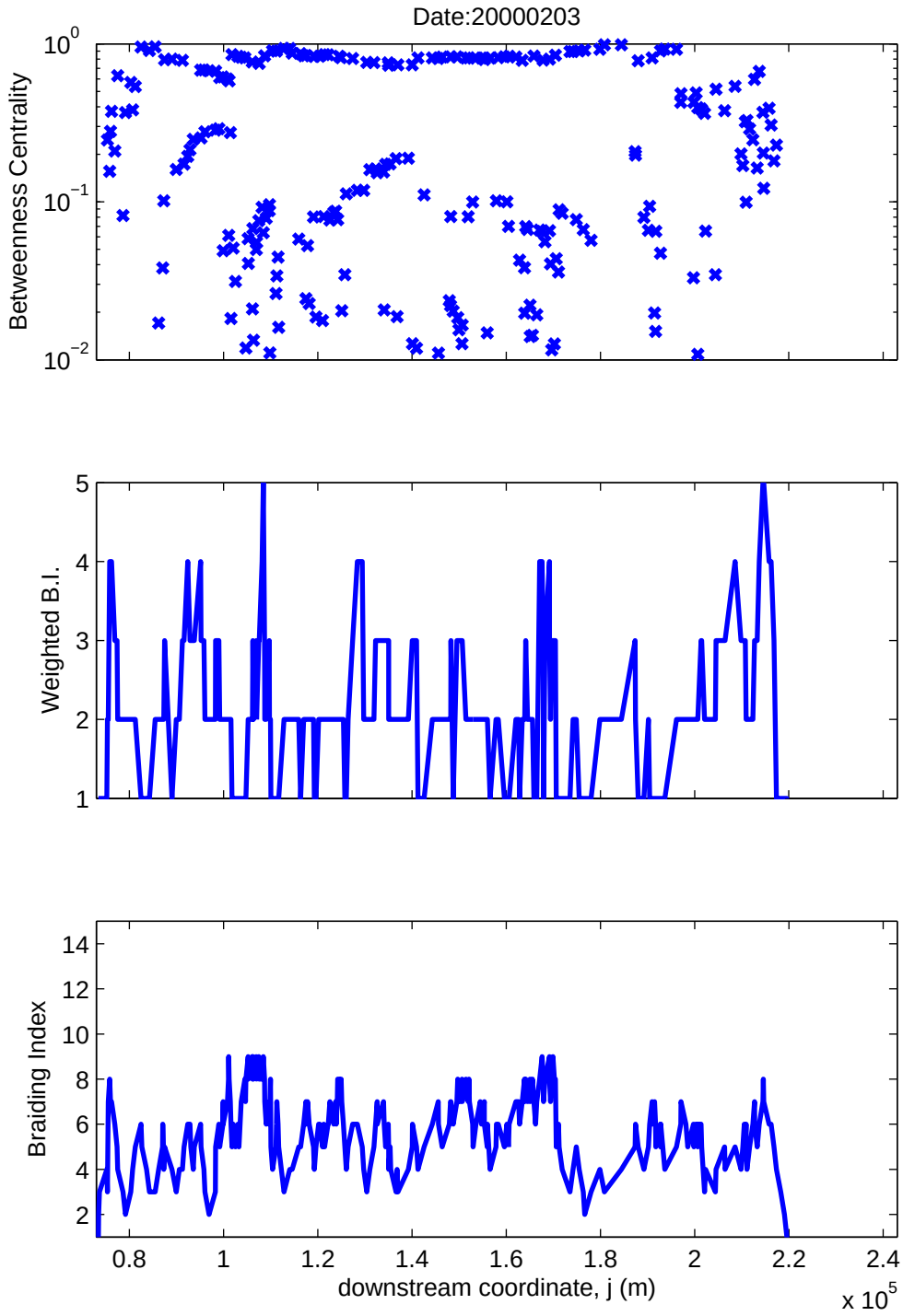

Figure 4.8 Braiding index, weighted braiding index and betweenness centrality along the channel network, date: 20000203

5 Discussion

5.1 Discussion of methods

5.1.1 River network extraction

The extraction of the river network from satellite images consists of multiple steps, involving both remote sensing and GIS techniques. First of all, there is the classification of the satellite images. The choice of using a tasselled cap transformation before classifying the image was made to make multiple scenes more consistent with each other. Other methods that were tried include supervised classification on the original satellite image using signature sets from the image space and unsupervised classification. Using a supervised classification with signature sets from the image space involved creating training areas in the satellite images. When using the Tasselled Cap transformed image, the classification signatures were successfully created from the feature space. The latter resulted in more pure classes and was less time-consuming to perform. Unsupervised classification yielded inconsistency between scenes, rendering this method inappropriate for analyses of the development between multiple scenes.

The second part of the network extraction is a series of GIS procedures yielding channel centrelines with channel widths. The channel centre pixels produced by the thinning algorithm (ArcGIS) needed some enhancements due to the large number of artefacts and errors. This algorithm was not primarily developed to extract river centrelines but for more regular features like roads or lines on a map, which is the main cause of these undesired results. An improved version of this algorithm would enhance this process. Effort is being put in the development of this algorithm (Joris Bak - ESRI NL, *Pers. Comm.*).

An overestimation of the channel width in narrow channels is introduced by the procedures used. The mean distance to the nearest bank of the centreline is used as channel width. When the centreline of a small channel is connected to the centreline of a larger channel, the end of the arc representing the channel lies within the larger channel (Fig. 5.1). The part of the narrow channel within the wider channel uses the distance to the bank of the wide channel for the calculation of the width. The width overestimation influences the bifurcation development, the asymmetry can be both higher as lower due to this effect depending whether the narrow channel is the largest or smallest channel of a bifurcation, respectively (note that the described overestimation of width occurs both at bifurcations as confluences). This effect subsequently affect the bifurcation asymmetry development. The effect on the latter is diminished by only linking two bifurcations between scenes when the connected channels have a comparable length, as the bifurcation asymmetries will have similar overestimation in both scenes, though the values are faulty.

Figure 5.1 Overestimation of channel width when a narrow channel is connected to a wide channel. At both ends of the highlighted channel (in red), the large distance to the nearest bank causes the width of this channel to be too high. This effect is larger for shorter channels.

5.1.2 Logical network generation

In the process of generating a logical network, the geographic topology of the river network as created by ArcGIS is converted to a network topology. The only variable in this process is the flow direction of the river to determine which end of an arc is upstream and which is downstream. In the current process, a general flow direction is assumed for the whole river. This works quite well for the current river since the flow direction is fairly constant. For more curved channels, a more sophisticated method should be used. Suggestions are: 1) projecting the coordinates to a curved axis or 2) deduce the flow direction from the network with a model by defining the most upstream and / or downstream nodes.

The logical network is enhanced by removing arcs which are shorter than half the width, because the meaning of such 'channels' is doubtful. The removal of these elements from the logical network resulted in complex nodes with trifurcations of even more connected channels. These nodes are excluded in the process of linking bifurcations between two scenes.

5.1.3 Network analysis

The network topology is finally rewritten to a connectivity matrix, in order to calculate network measures. In the river network, multiple arcs can connect to the same two nodes. In a connectivity matrix, only one connection is possible between two nodes, this is a inherent property of the connectivity matrix. The only way to include multiple channels in the network analyses is to address this in the weight. In the current methods, the mean length and the sum of the width of multiple channels connecting the same node was used as weights for that connection. A data structure which allows multiple connections between two nodes is preferred over the connectivity matrix, this is not used in the current study as the used network analysis toolbox requires a connectivity matrix.

The network measures are calculated using the Brain Connectivity Toolbox, a toolbox developed by neurologists. The network measures in this toolbox are universal and originated from a wide scope of disciplines. Many measures are available to analyse complex networks, but the network of rivers is relative simple. Therefore many measures have no use in river morphology as they do not represent a physical property of the river. Besides a better data structure to store the network, as described in the previous paragraph, the network analysis methods should be tailored to specifically analyse river networks. This

is beyond the scope of the current research, but it is shown in this study that network analysis is a powerful tool for river morphologists.

5.1.4 Bifurcation development

The development of bifurcation asymmetry is assessed by comparing the bifurcation asymmetry between the same bifurcation in two different scenes. The bifurcation in two scenes are linked to each other based on distance and angle of the downstream connected channels. Nevertheless, erroneous linked nodes exist, but these are in minority. The bifurcation asymmetry in smaller channels is influenced by the overestimation of channel width as described in section 5.1.1. This effect is diminished by only using bifurcations of which the connected channels have comparable lengths.

Theoretically, the bifurcation asymmetry should be calculated from the discharges. Since discharge data is not known for all individual channels and not derivable from satellite images in this case, channel widths were used. Channel width scales more or less with discharge, but deviations exist (for example areas with stagnant water). In the analysis of bifurcation asymmetry development, discrepancies in the width-discharge relation have less effect: If for one bifurcation the ratio of channel widths changes, this is most likely the effect of a change in discharge distribution.

Assessing the bifurcation asymmetry development has not been successful for all scenes. This happens when the changes between two scenes are too big due to a morphological development or by a change in appearances as a result of a change in water stage. In such periods, the bifurcation asymmetry appears chaotic, this is either due to a large morphological change or the result of errors in linking the bifurcations between two scenes. Scenes taken short after each other with low differences in discharge were the most useful for linking bifurcations and assessing the bifurcation asymmetry development.

5.1.5 Weighted braiding index

The calculation of the proposed weighted braiding index (wBI) is based on an educated guess for channel importance: if the betweenness centrality / importance of a channel is higher than half (0.5) of the theoretical betweenness of a channel when all channels in the cross section are equally important, it is counted in the wBI. The resulting wBI is lower for reaches with dominant channel formation as intended, but the choice of this equation, especially the value 0.5, is arbitrary.

5.2 Discussion of results

5.2.1 Interpretation of network measures

As discussed before, only a few network measures have a potential physical meaning in terms of river morphology. Only the betweenness centrality, clustering coefficient and modularity were used. In the end, only the betweenness centrality is a useful measure. The clustering coefficient is too limited to identify clusters in a river. The modularity could be a useful measure to identify distinct branches in the river, but the river network has a limited variation to successfully identify such branches. Adjusting the network analysis methods to suit river networks could result in other useful measures for rivers.

5.2.2 River network evolution

The braiding index of the river shows a clear stage and seasonal dependency, in agreement with *Alabyan and Chalov* (1998). The seasonal dependency consist of a decreasing braiding index during low stages and an increasing braiding index after floods. The stage dependency was expected to show a lower braiding index during high water stages due to the submergence of bars. The latter effect is not present in the data as the used dataset does not include extreme discharges with bar-full conditions, therefore this hypotheses is not tested.

During constant flow conditions, bifurcations will become more asymmetrical or one of the two branches will close (*Bolla Pittaluga et al.*, 2003; *Kleinhans et al.*, 2008). In a period of constant low flow conditions, the braiding index and the weighted braiding index decreased. The first is the result of closing bifurcations, the latter is also influenced by the development of a dominant channel, thus the development of bifurcation asymmetry.

In the used dataset, there were two sets of scenes which fell within the same season with comparable low-discharge conditions. During one of these periods, the largest part of the bifurcations showed a slight increase of bifurcation asymmetry, a decrease of braiding index and weighted braiding index as hypothesised. In the other period there was hardly any development noticed, but there was almost no development of bifurcation asymmetry and dominant channel possible as both the braiding index as the weighted braiding index were already very low. In the whole analysed period, the braiding index was the lowest in the dry seasons and there was a significant development of a dominant channel in these scenes as the weighted braiding index dropped to 2 or lower. The (weighted) braiding index increases during high discharge conditions, but no clear decrease in bifurcation asymmetry is noticed; a chaotic development was observed. Discharge peaks cause channels to be reactivated and discharge to be spread more evenly. These changes caused by discharge peaks are dominated by large changes rather than a gradual decrease of bifurcation asymmetry.

Huang et al. (2004) explained the exitance of multiple channels using a sediment transport optimisation theory, in their theory it is more efficient for a river with a high sediment load to transport the sediment over two or more channels. The results of the current research shows that bifurcations become more asymmetrical under steady flow conditions effectively decreasing the braidingness of the river. The existence of a braided pattern is maintained by flooding when abandoned channels are reactivated and new channels are formed, but the existence of multiple channels is not the stable state of the river as they gradually disappear after the flood. The existence of multiple channels corresponds with theories about the formations of bars. Braided bars will form under the water table during high water stages in rivers with a high width-to-depth ratio (*Crosato and Mosselman*, 2009; *Marra*, 2008). This pattern is revealed when the water level drops, this corresponds with the results of this research, as a highly braided pattern is observed after flood peaks.

6 Conclusions

6.1 Development of methods

A method was developed to extract the river channel network from satellite imagery. The resulting channel network dataset contains the width and length of every channel segment. This dataset was transposed to contain a network topology, which contains information about the connectivity of all elements. From this dataset, a connectivity matrix was derived which was used for network analysis. The successful applications of network analysis methods shows that branched rivers can be analysed as a network and this can be a valuable tool in river morphology research and engineering.

From the channel network, the braiding index for the whole river and every cross section and the bifurcation asymmetry for every bifurcation were successfully calculated. The connectivity matrix was used to calculated network measures, most important the betweenness centrality of nodes and arcs which is a measure for the importance of these elements in the network. The betweenness centrality is the basis of the weighted braiding index which is a measure of dominant channel formation.

From a set of channel network of two scenes, the bifurcation asymmetry development of individual bifurcations was addressed. From a range of channel networks with associated properties, it is possible to gain detailed insight in the development of the river.

6.2 Network analysis

The betweenness centrality is a network measure calculated for all elements in the river networks. This measure successfully maps the importance of different elements in the network. The betweenness centrality is calculated from the width and length of individual channel segments and, most important, the whole up- and downstream network configuration are taken into account. Such approach corresponds with reality as changes in a river affect both up- and downstream elements in the channel network.

Other network measures which were thought to be potentially useful are the clustering coefficient for identifying braided reaches and modularity to identify distinct subnetworks. Both measures where not useful as these measures produced undesired results, possibly due to the limitations of the current used (Neurological) toolbox.

6.3 River evolution

During persistent steady low flow conditions a dominant channel forms in a braided river due to the development of bifurcation asymmetry and closures of bifurcations. The braid-

ing index decreases due to the closure of bifurcations. The Jamuna river is not actively braiding at the end of the dry season, as there are parts of the river with only one dominant channel.

As a result of discharge peaks, discharge is spread more evenly between channels, abandoned channels are reactivated and new channels are formed. This increases the braiding index of the river and decreases the presence of one or only a few dominant channels. The presence of multiple parallel channels is the result of discharge peaks, but the rivers develops to have a single active thread in absence of floods.

Changes in the appearance of the channel pattern rather than actual morphological development due to differences in water height were noticed as scenes with high water stage differences showed too less resemblance with the previous or next scene in a succession to successfully link the objects in these scenes. A decrease of (apparent) braiding index during high discharge condition due to the submergence of bars was not observed in the data used, as bar-full discharge conditions are not present in the used dataset.

7 Future work

This chapter contains a few ideas for future studies based on the same methods which were not incorporated or completed during the current study.

7.1 Island / bank composition

Valuable information on the origin of islands in the river can be derived from their composition. Young fluvial bars consist of bare sediment, while floodplains are cultivated or are grown with vegetation. The incorporation of this information into the network dataset can give information about how the island was formed and can be used to discriminate braided from anastomosing processes. The age of bars could be evaluated by evaluating the period a bar was present in previous satellite images.

To distinguish between floodplain-islands (anabranching) and fluvial bars (braiding), the behaviour of these objects (bar / island) during flood is important since the largest objects are only inundated during the highest water levels. When the object migrates, it is most likely a fluvial bar and a floodplain otherwise. The activity of an object in the river can be addressed using change detection remote sensing techniques. The classification can be aided with the use of shape-based image classification and elevation data, since fluvial bars and floodplains could have a different shape.

7.2 Advanced network analysis

The network analysis toolbox used for this study features a broad range of network measures. However, only one of them has been useful for river network analysis (the betweenness centrality). Other network measures could be useful like the clustering coefficient to gain more knowledge in the braiding structure or the network modularity to asses distinct regions in the network. However, these measures did not produce a satisfactorily result due to the large difference in in topology of a river network and neurological or social networks where these measures were designed for.

The current study showed that network analysis is a useful tool in river morphological research. The next step is to make the methods more suitable to analyse rivers in contrary to using methods developed for other fields of study. Network analysis methods designed for rivers will circumvent limitations and assumptions which are invalid for rivers.

References

Alabyan, A. M., and R. S. Chalov (1998), Types of river channel patterns and their natural controls, *Earth Surf. Process. Landforms*, *23*(5), 467–474, doi:10.1002/(SICI)1096-9837(199805)23:5%3C467::AID-ESP861%3E3.0.CO;2-T.

Barrat, A., M. Barthelemy, R. Pastor-Satorras, and A. Vespignanni (2004), The architecture of complex weighted networks, *Proc. Nat. Acad. Sci. USA*, *101*(11), 3747–3752, doi:10.1073/pnas.0400087101.

Bertoldi, W., L. Zanoni, and M. Tubino (2009a), Planform dynamics of braided streams, *Earth Surf. Process. Landforms*, *34*(4), 547–557, doi:10.1002/esp.1755.

Bertoldi, W., L. Zanoni, S. Miori, R. Repetto, and M. Tubino (2009b), Interaction between migrating bars and bifurcations in gravel bed river, *Water Resour. Res.*, *45*, W06418, doi:10.1029/2008WR007086.

Bolla Pittaluga, M., R. Repetto, and M. Tubino (2003), Channel bifurcation in braided rivers: Equilibruim configurations and stability, *Water Resour. Res.*, *39*(3), WR001112, doi:10.1029/2001WR001112.

Bridge, J. (1993), The interaction between channel geometry, water flow, sediment transport and deposition in braided rivers, in *Braided Rivers*, edited by J. Best and C. Bristow, pp. 13–71, Geolocial Society, London, Special Publication 75, isbn:0903317931, doi:10.1144/GSL.SP.1993.075.01.02.

Chander, G., B. L. Markham, and D. L. Helder (2009), Summary of current radiometric calibration for Landsat MSS, TM, ETM+ and EO-1 ALI sensors, *Remote Sens. Environ.*, *113*(5), 893–903, doi:10.1016/j.rse.2009.01.007.

Crist, E. P. (1985), A TM Tasseled Cap equivalent transformation for reflectance factor data, *Remote Sens. Environ.*, *17*(3), 301–306, doi:10.1016/0034-4257(85)90102-6.

Crosato, A., and E. Mosselman (2009), Simple physical-based predictor for the number of river bars and the transition between meandering and braiding, *Water Resour. Res.*, *45*(3), W03424, doi:10.1029/2008WR007242.

Egozi, R., and P. Ashmore (2008), Defining and measuring braiding intensity, *Earth Surf. Process. Landforms*, *33*(14), 2121–2138, doi:10.1002/esp.1658.

ESRI (2008), *ArcGIS Desktop 9.3 Help*.

Euler, L. (1741), Solutio problematis ad geometriam situs pertinentis (The solution of a problem relating to the geometry of position), *Commentarii academiae scientiarum Petropolitanae*, *8*, 128 – 140.

Ferguson, R. (1987), Hydraulic and sedimentary controls of channel pattern, *River Channels: Environment and Process*, pp. 129–158.

Fletcher, D. (1987), Modelling GIS transportation networks, http://ecow.engr.wisc.edu/cgi-bin/getbig/cee/659/adams/readings/dynamicseg/fletcher.pdf.

Freeman, L. (1987), Centrality in Social Networks Conceptual Clarification, *Social Networks*, *1*(3), 215–239, doi:10.1016/0378-8733(78)90021-7.

Huang, C., B. Wylie, C. Homer, and G. Zylstra (2002), Derivation of a Tasseled Cap Transformation Based on Landsat 7 at-Satellite Reflectance, *Int. J. Remote Sens.*, *23*(8), 1741–1748, doi:10.1080/01431160110106113.

Huang, H. Q., H. H. Chang, and G. C. Nanson (2004), Minimum energy as the general form of critical flow and maximum flow efficiency and for explaining variations in river channel pattern, *Water Resour. Res.*, *40*, W04502, doi:10.1029/2003WR002539.

Jagers, H. R. A. (2003), Modelling Planform Changes of Braided Rivers, Ph.D. thesis, Twente University, http://purl.org/utwente/41419.

Jerolmack, D. J., and D. Mohrig (2007), Conditions for branching in depositional rivers, *Geology*, *35*(5), 463–466, doi:10.1130/G23308A.1.

Kleinhans, M. G., and J. H. van den Berg (2010), River channel and bar patterns explained and predicted by an empirical and a physis-based method, *Earth Surf. Process. Landforms*.

Kleinhans, M. G., H. R. A. Jagers, E. Mosselman, and C. J. Sloff (2008), Bifurcation dynamics and avulstion duration in meandering rivers by one-dimensional and three dimensional models, *Water Resour. Res.*, *44*, W08454, doi:10.1029/2007WR005912.

Knighton, A. D., and G. C. Nanson (1993), Anastomosis and the continuum of channel pattern, *Earth Surf. Process. Landforms*, *18*(7), 613–625, doi:10.1002/esp.3290180705.

Knighton, D. (1984), *Fluvial Forms and Processes*, Arnold London, isbn:0713164050.

Leopold, L. B., and M. G. Wollman (1957), River Channel Patterns: Braided, Meandering and Straight, *Geol. Survey Prof. Paper*, *282-B*, 39–85.

Leopold, L. B., and M. G. Wolman (1960), River meanders, *Geol. Soc. Am. Bull.*, *71*, 769–793, doi:10.1130/0016-7606(1960)71[769:RM]2.0.CO;2.

Lillesand, T. M., R. W. Kiefer, and J. W. Chipman (2007), *Remote sensing and image interpretation*, 6th ed., John Wiley & Sons New York, isbn:9780470052457.

Makaske, B. (2001), Anastomosing rivers: a review of their classification, origin and sedimentary products, *Earth Sci. Rev.*, *53*(3-4), 149–196, doi:10.1016/S0012-8252(00)00038-6.

Marra, W. A. (2008), Dynamics and interaction of bars in rivers and the relation between bars and a braided river pattern, BSc thesis., Dep. of Physical Geography, Fac. of Geosciences, Utrecht University (The Netherlands).

Nanson, G. C., and A. D. Knighton (1996), Anabranching Rivers: Their Cause, Character and Classification, *Earth Surf. Process. Landforms*, *21*(3), 217–239, doi:10.1002/(SICI)1096-9837(199603)21:3%3C217::AID-ESP611%3E3.3.CO;2-L.

Newman, M. (2008), The physics of networks, *Phys. Today*, *61*(11), 33, doi:10.1063/1.3027989.

Newman, M. E. J. (2003), Mixing patterns in networks, *Phys. Rev. E*, *67*(2), 26,126, doi:10.1103/PhysRevE.67.026126.

Newman, M. E. J. (2006), Finding community structure in networks using the eigenvectors of matrices, *Phys. Rev. E*, *74*(3), 36,104, doi:10.1103/PhysRevE.74.036104.

Nikora, V. I., and V. B. Sapozhnikov (1993), River network fractal geometry and its computer simulation, *Water Resour. Res.*, *29*(10), 3569–3575, doi:10.1029/93WR00966.

Parker, G. (1976), On the cause and characteristic scales of meandering and braiding in river, *J. Fluid Mech.*, *76*(3), 457–480, doi:10.1017/S0022112076000748.

Rubinov, M., and O. Sporns (2009), Complex network measures of brain connectivity: Uses and interpretation, *NeuroImage*, doi:10.1016/j.neuroimage.2009.10.003.

Schumm, S. (1985), Patterns of alluvial rivers, *Annu. Rev. Earth Planet. Sci.*, *13*(1), 5–27, doi:10.1146/annurev.ea.13.050185.000253.

Sporns, O. (2002), Graph Theory Methods For The Analysis Of Neural Connectivity Patterns, in *Neuroscience Databases: a practical guide*, edited by R. Kotter, chap. 12, pp. 169–183, Kluwer Academic Publishers, isbn:1402071655.

Strogatz, S. H. (2001), Exploring complex networks, *Nature*, *410*(6825), 268–276, doi:10.1038/35065725.

Struiksma, N., and G. J. Klaassen (1988), On the threshold between meandering and braided, in *International Conference on River Regime*.

Struiksma, N., K. Olesen, C. Flokstra, and H. de Vriend (1985), Bed deformation in curved alluvial channels, *J. Hydraul. Res.*, *23*(1), 57–79.

USGS (2008), Imagery for Everyone: Timeline set to release entire USGS Landsat archive at no charge Technical Announcement, - http://landsat.usgs.gov/documents/USGS_Landsat_Imagery_Release.pdf.

Van den Berg, J. H. (1995), Prediction of alluvial channel pattern of perennial rivers, *Sedimentology*, *12*(12), 259–279, doi:10.1016/0169-555X(95)00014-V.

Appendix A | Content of hard disk

The folder \Data contains the (pre-processed) satellite images, \Classified contains classified satellite images and the required intermediate images, \Networkextraction contains the data which are produced by the channel extraction process. The developed ArcGIS toolbox is available in the folder \Toolboxes, Automated Python versions of these scripts and the scripts for satellite images pre-processing are available in \Scripts. The folder \Matlab contains data, scripts and plots used for network generation and network analysis. The folder \Thesis contains the text, images and other material of this thesis.

In the following list of the data structure, long lists of files are abbreviated by a short description and sequences of files are listed with placeholders: yyyymmdd denote different dates, mmm different months, sat and sen denote different satellites and sensors.

```
\Classified
  \Supervised
  \TassCap
    TC_yyyymmdd_se.tif
    \Classified
      yyyymmdd.img
    \FeatureSpace
      yyymmmdd_n_m.fsp.img
    \Model
      tasseledcap_sen.gmd
      TC_yyymmdd_se.mdl
      generatemodels.m
    \Signatures
      FS_se_mmm

\Data
  \Landsat
    \Composite
      \p---
        \r---
          yyyymmdd_sat-DNs.tiff
          yyyymmdd_sat-rad.tiff
          yyyymmdd_sat-ref.tiff
    \RAW Data
      \Folders per scene
        TIFF image per band
        txt files with header data
```

```
  \JamunaDischarge

\Matlab
  startup.m  - imports data in mat files to the workspace and sets paths to functions
  \BCT
    various.m-files
  \Data
    yyyymmdd.xlsx
    aat, aat_netw.xls
    net, nat_netw.xls
    data.mat
    discharge.mat
    fromto.mat
    netw.mat
    netwprop.mat
    netwproparcs.mat
    ts.mat
  \Functions
    - functions starting with build_ are used for generating and linking the network
    - functions starting with export_ are used to export arc and node properties
    - functions starting with plot_ are used to display data
  \Plots
    - generated plots are saved here
  \Scripts
    Scripts which are used for batch processing multiple datasets,
     - these scripts call functions from the functions folder

\Networkextraction
  \01CleanClassified
    Clean_yyyymmdd.img
  \02SelectedObjects
    Channel_yyyymmdd_u.img
    NotChannel_yyyymmdd_u.img
  \03Centerlines
    centerlines_yyyymmdd.shp
    centerlines_yyyymmdd_e.shp
  \04ChannelWidth
    Distance_yyyymmdd.img
    wdth_yyyymmdd.shp
  \05ChannelNetwork
    netw_yyyymmdd
    midp_yyyymmdd
  \06Database
    yyyymmdd.mdb
  \99BridgeMask
    bridge.shp
    bridge_mask.img

\Script
  CalibrationCoefConverter.xlsx
  Landsat2Composite.py
  \NetworkExtraction
```

```
    01,02,03,04,05,06.py
     - these Python scripts are exports of the created ArcGIS toolbox
    Autom_CenterlineExtration.py
    Autom_NetworkGeneration.py
     - these scripts are combined and automated versions of the loose scripts


\Thesis
  \AdditionalMaterial
  \Appendices
  \Conferences
  \Literature
  \Presentations
  \researchproposal
  \thesis

\Toolboxes
  NetworkExtrationtoolbox.tbx
     - ArcGisToolbox containing the following scripts:
        01_Select water from Classified image
        02_Extract Centerline
        03_Manually edit centerlines
        04_Update Channel Width
        05_Create Coverage
        06_Build Network and add to Geodatabase
```

Appendix B | Bifurcation asymmetry plots all (intra-annual) autumn and winter scenes

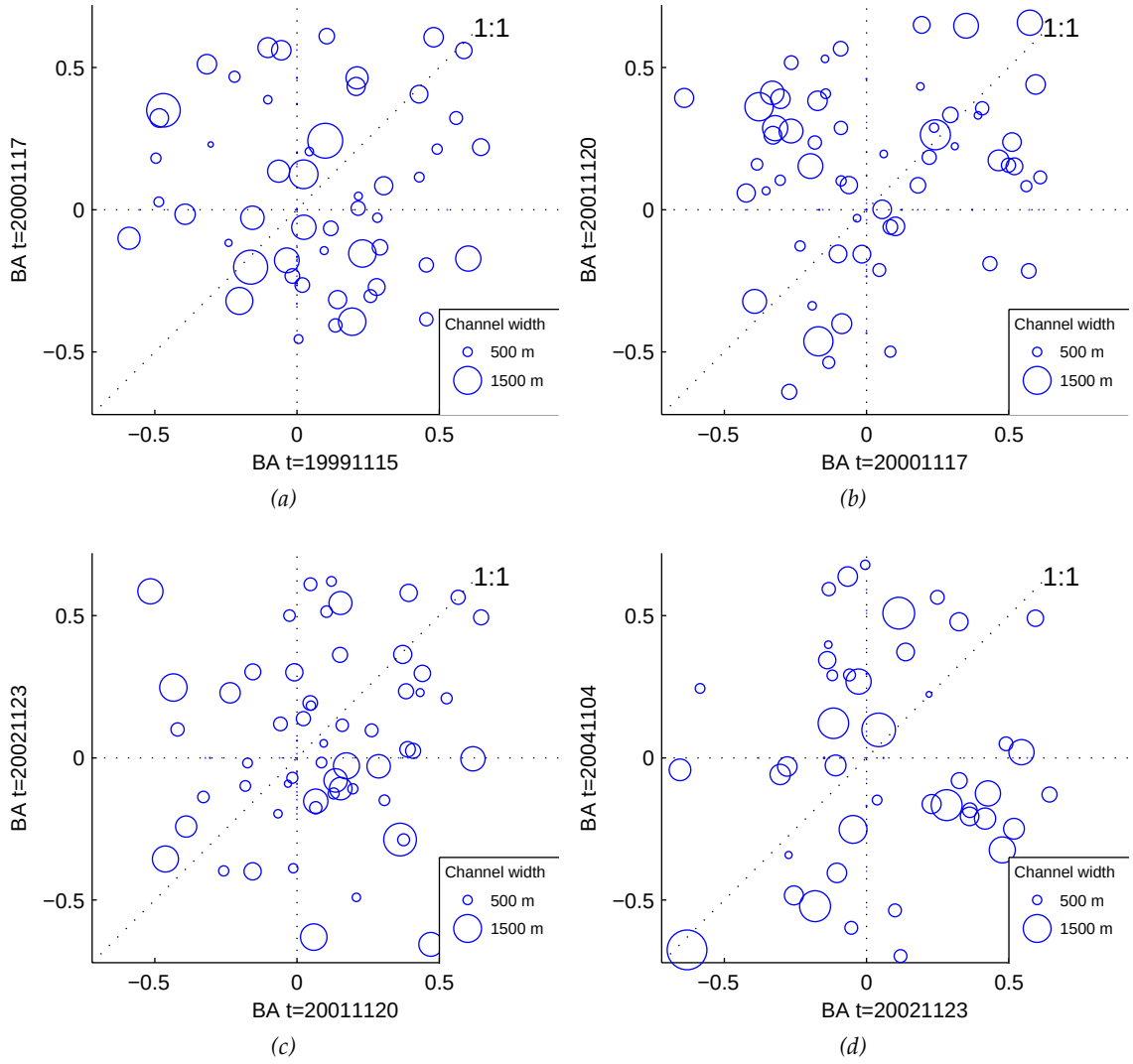

Figure B.1 Bifurcation asymmetry development for all autumn scenes. See Fig. 3.8 for interpretation of plots.

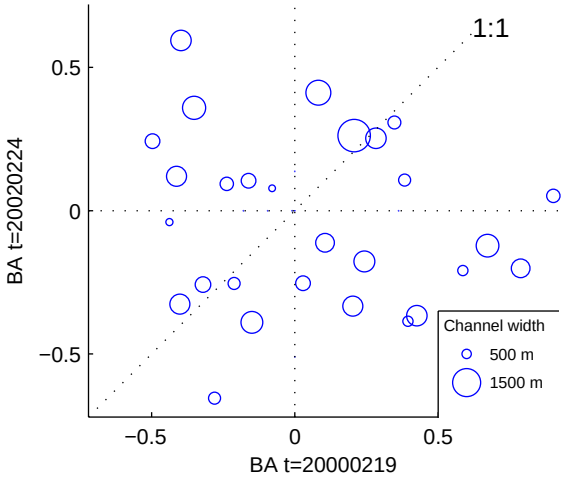

(a)

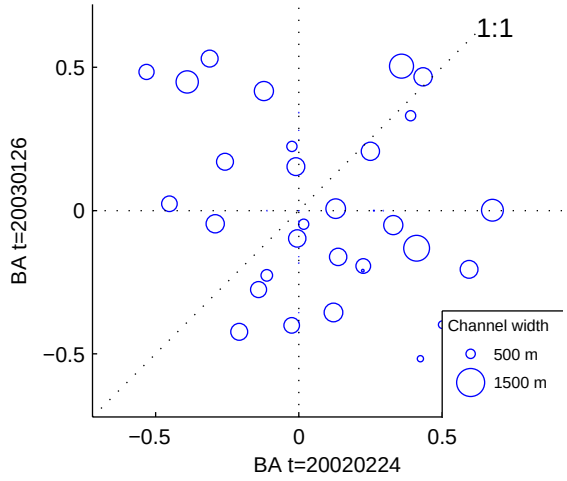

(b)

Figure B.2 Bifurcation asymmetry development for all winter scenes. Consecutive scenes from the same year are not present in this figure. See Fig. 3.8 for interpretation of plots.

Appendix C | Betweenness centrality, braiding index and weighted braiding index for all scenes

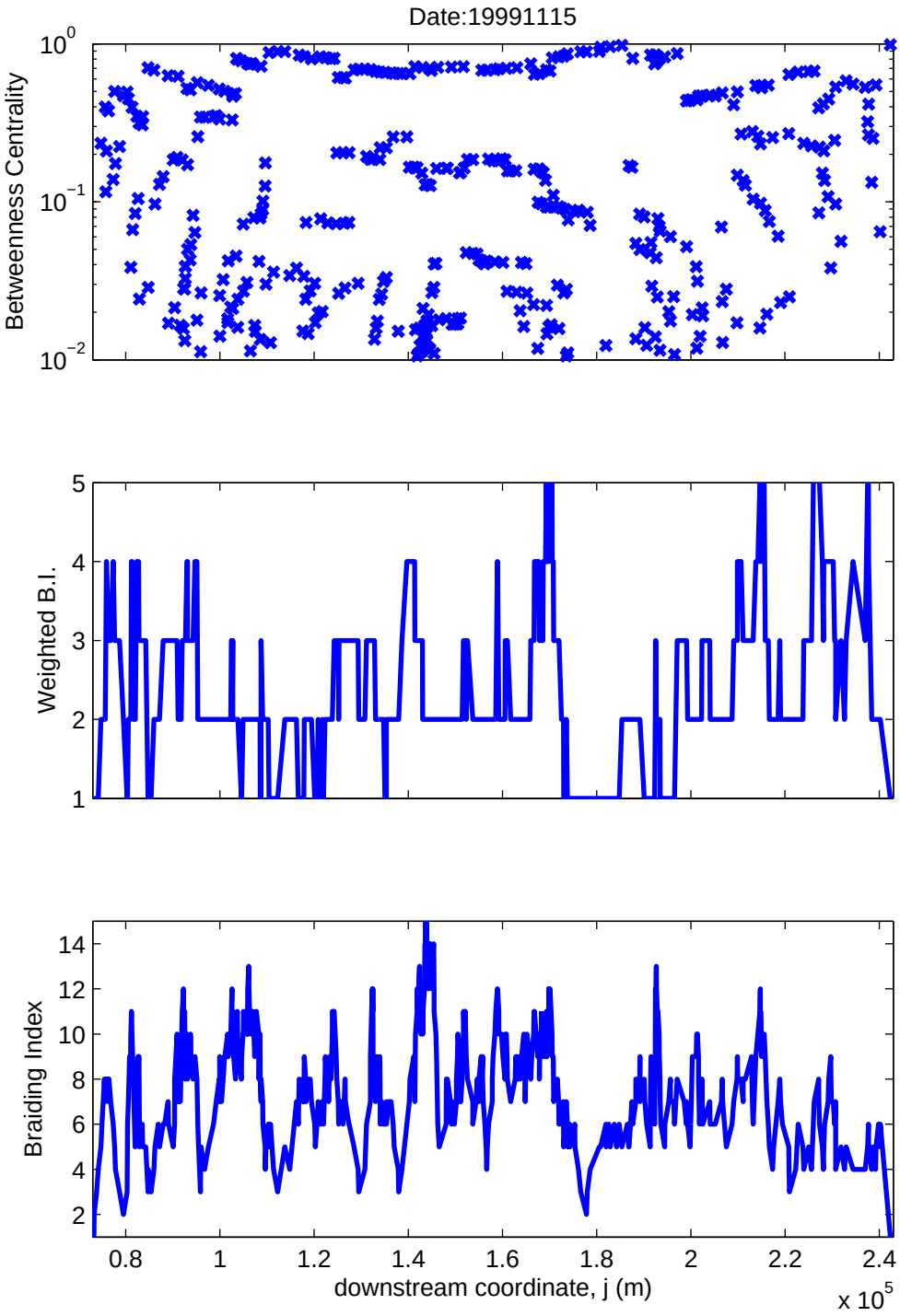

Figure C.1 Braiding index, weighted braiding index and betweenness centrality along the channel network, date: 19991115

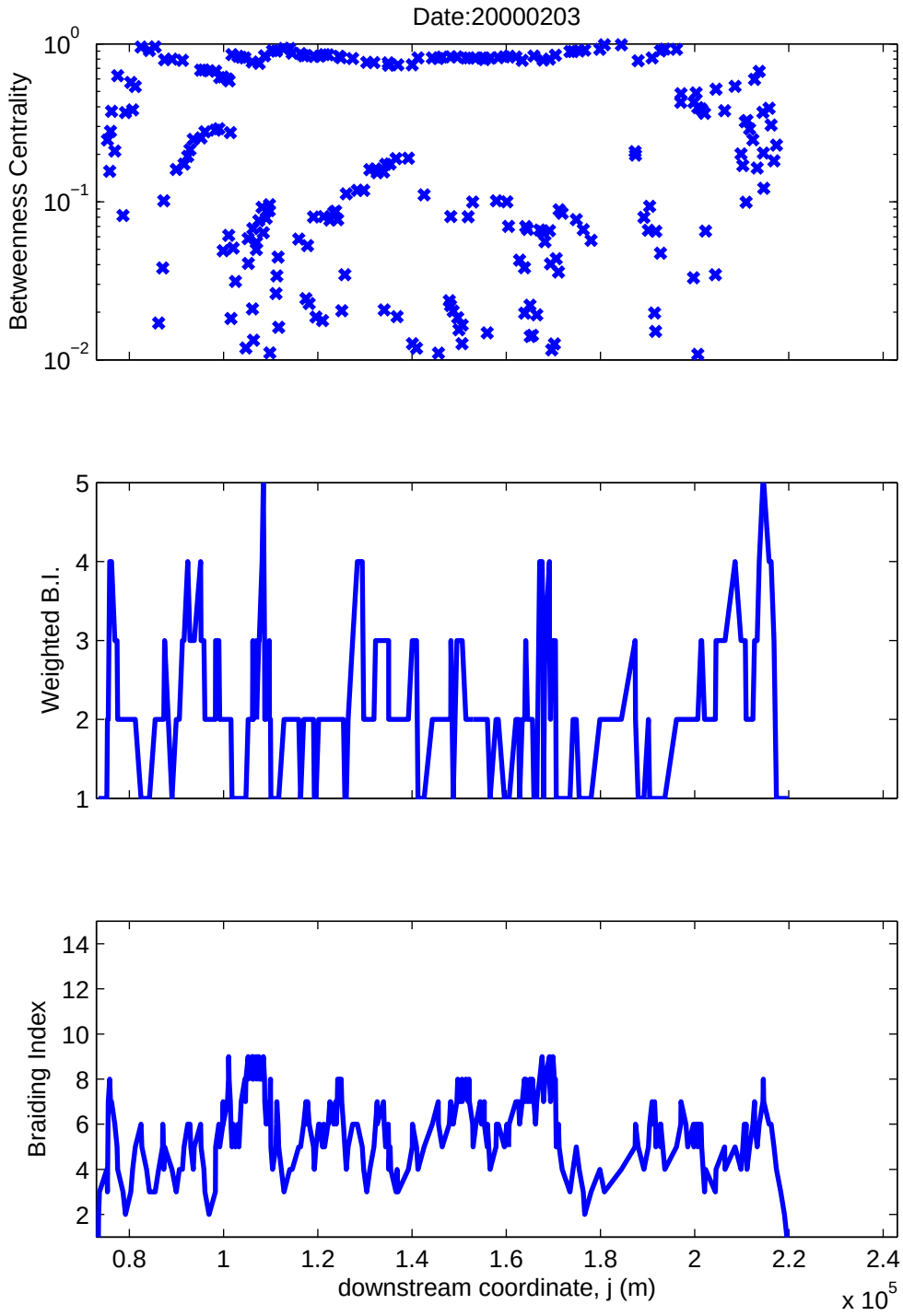

Figure C.2 Braiding index, weighted braiding index and betweenness centrality along the channel network, date: 20000203

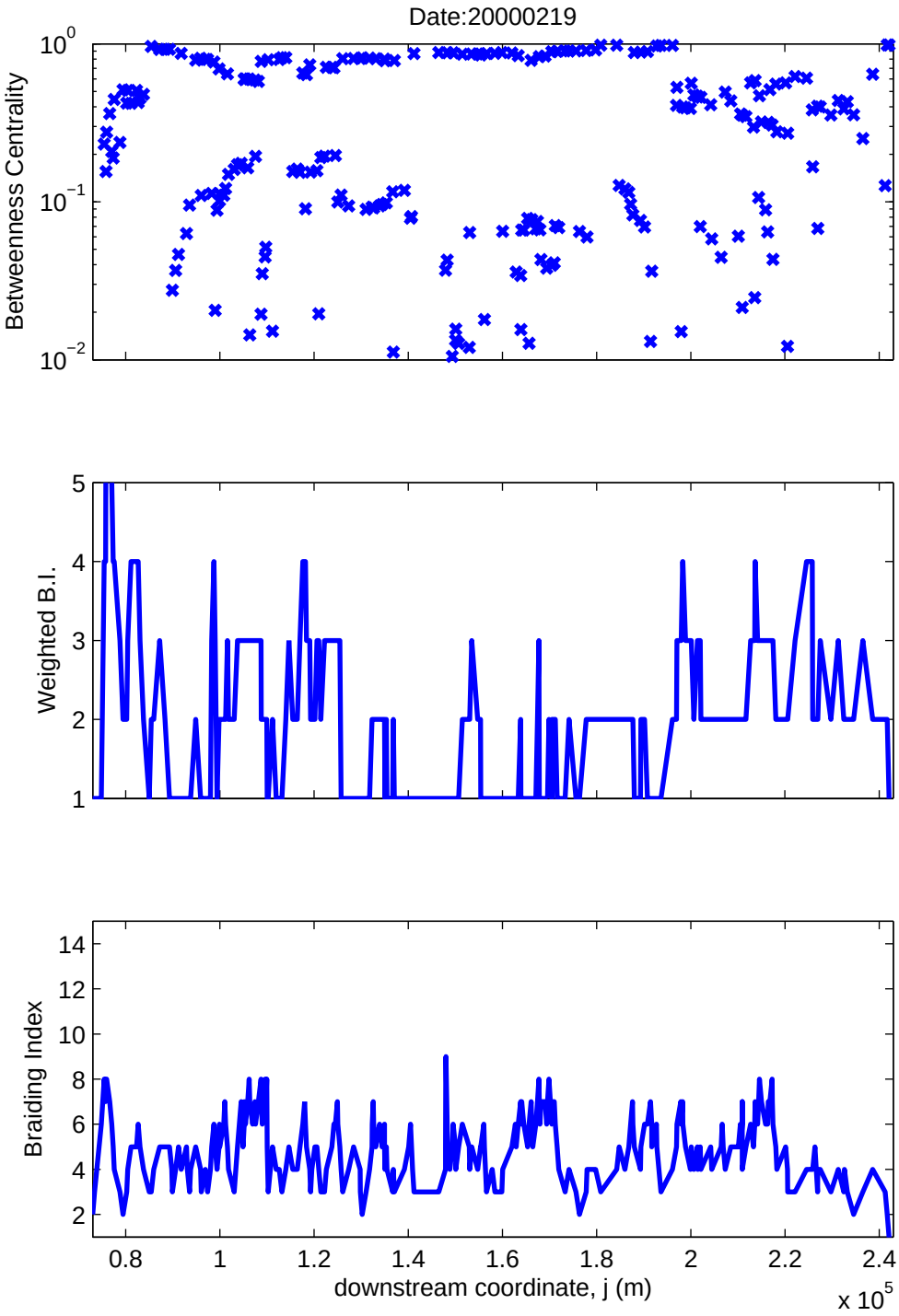

Figure C.3 Braiding index, weighted braiding index and betweenness centrality along the channel network, date: 20000219

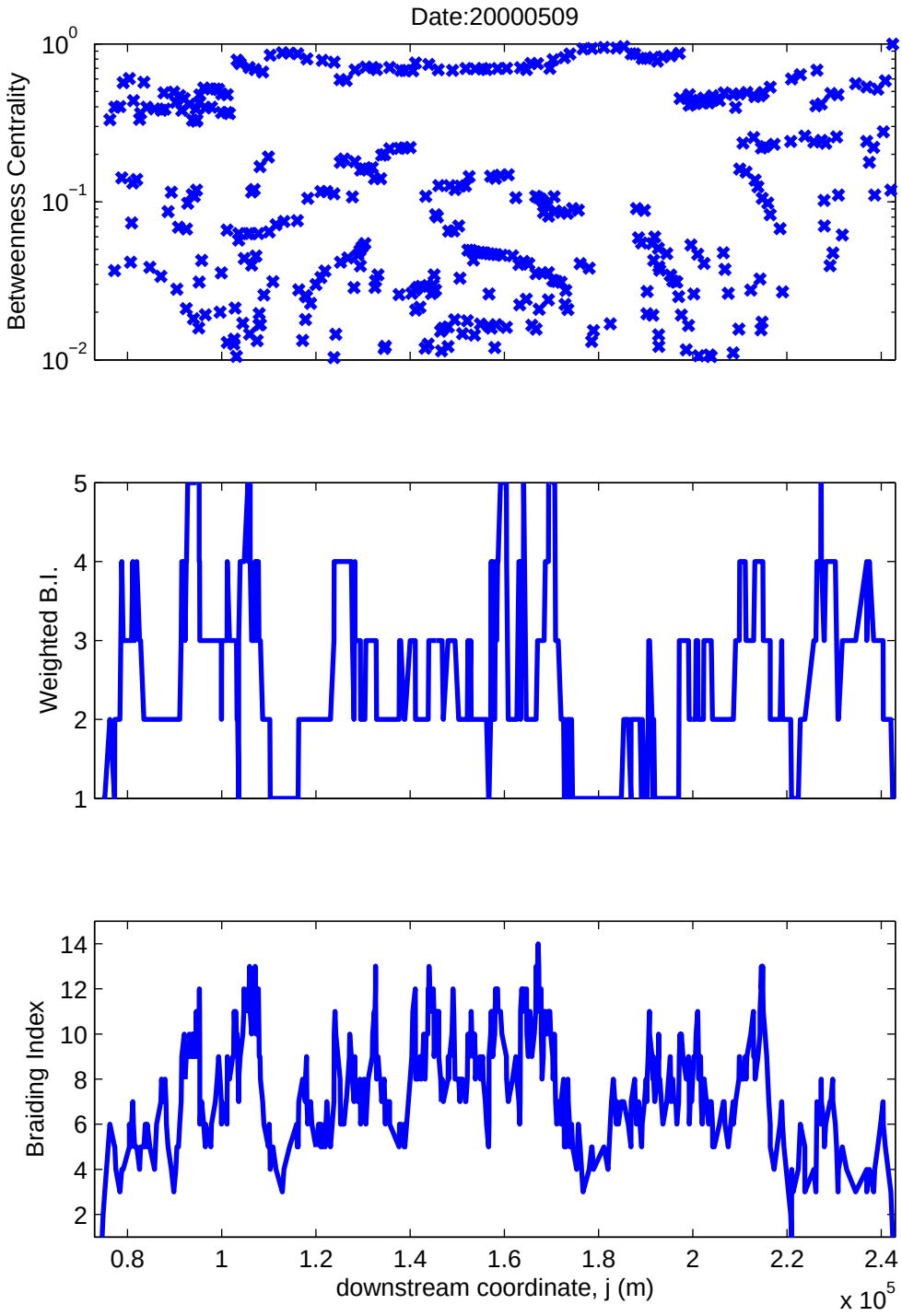

Figure C.4 Braiding index, weighted braiding index and betweenness centrality along the channel network, date: 20000509

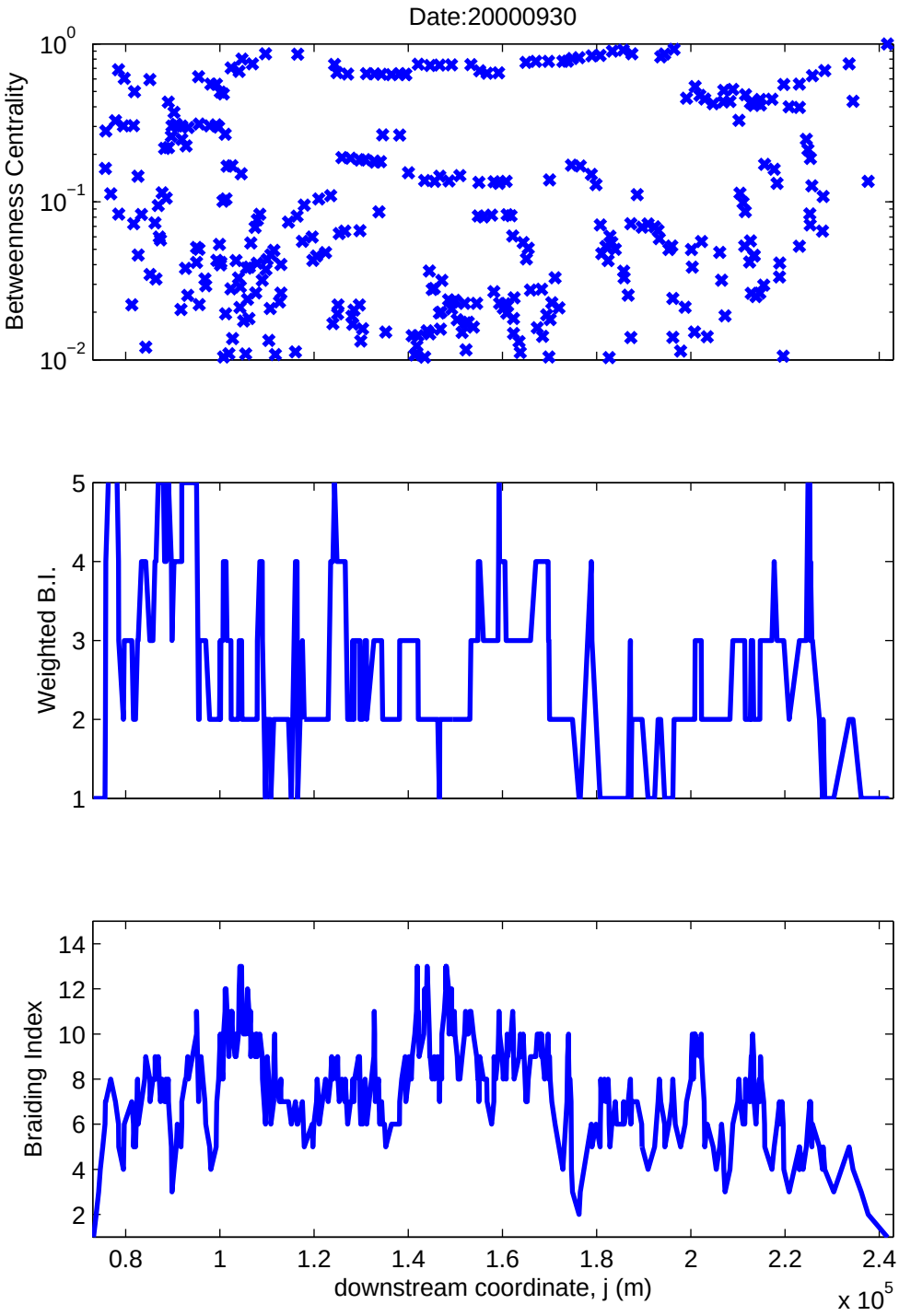

Figure C.5 Braiding index, weighted braiding index and betweenness centrality along the channel network, date: 20000930

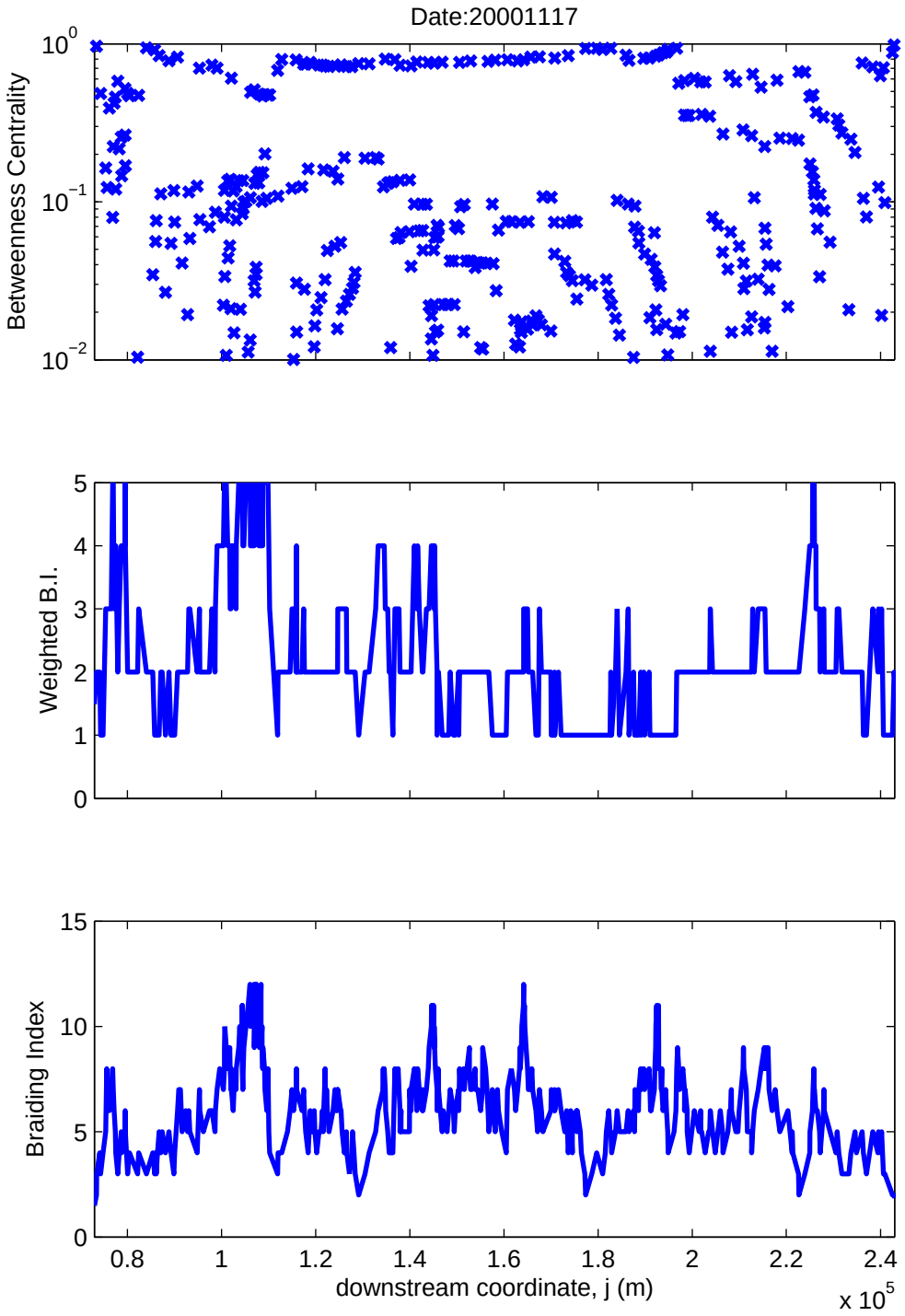

Figure C.6 Braiding index, weighted braiding index and betweenness centrality along the channel network, date: 20001117

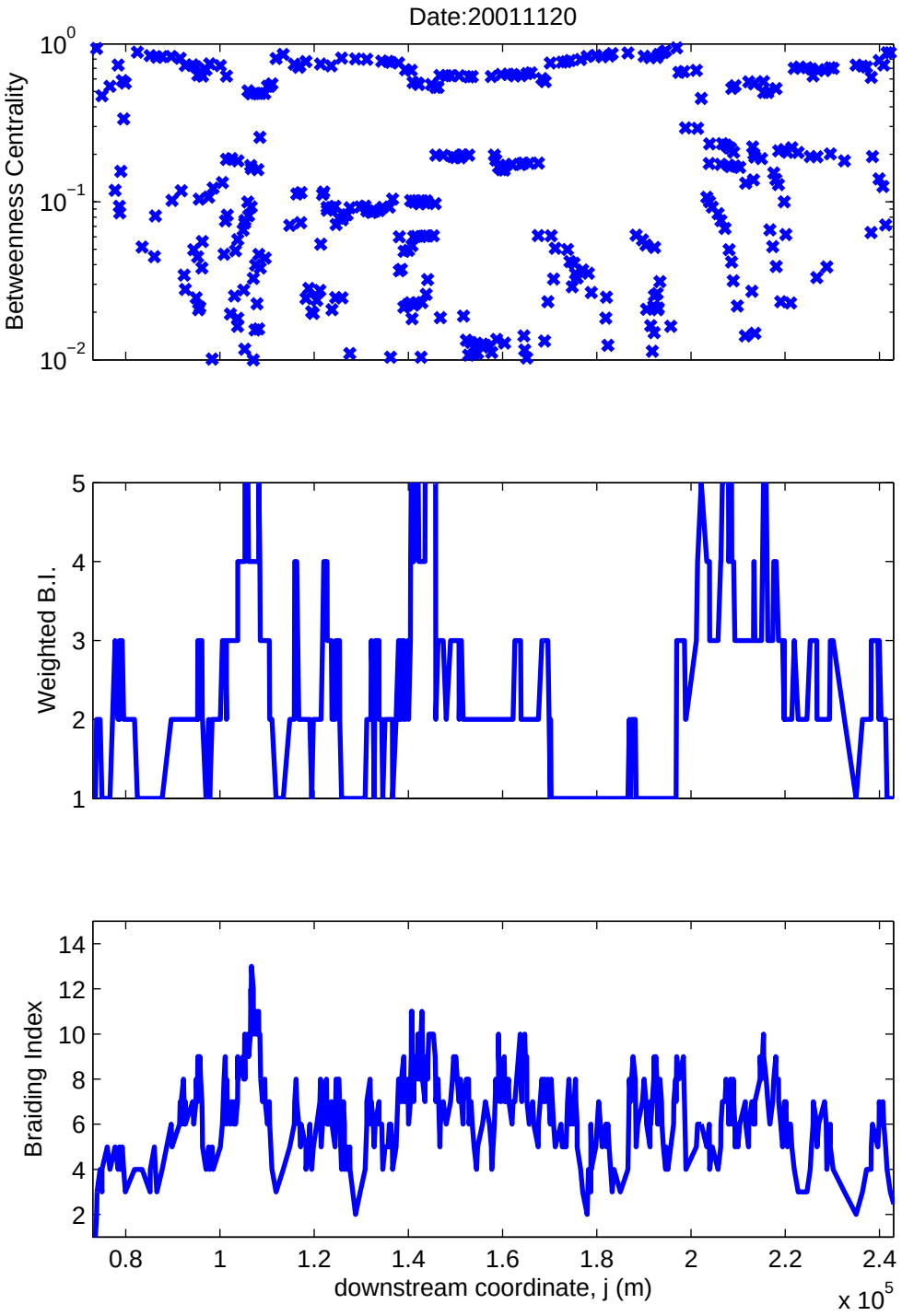

Figure C.7 Braiding index, weighted braiding index and betweenness centrality along the channel network, date: 20011120

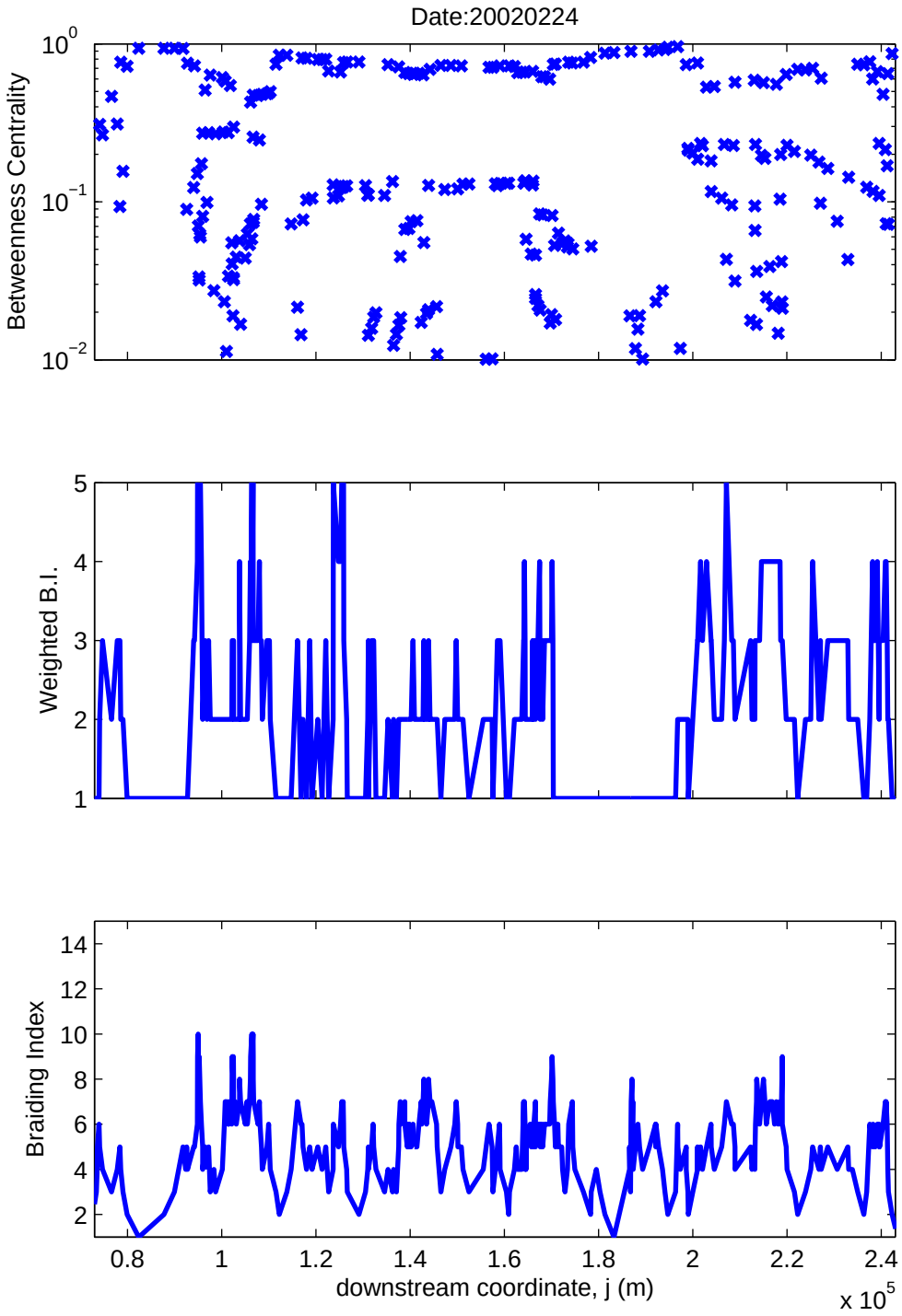

Figure C.8 Braiding index, weighted braiding index and betweenness centrality along the channel network, date: 20020224

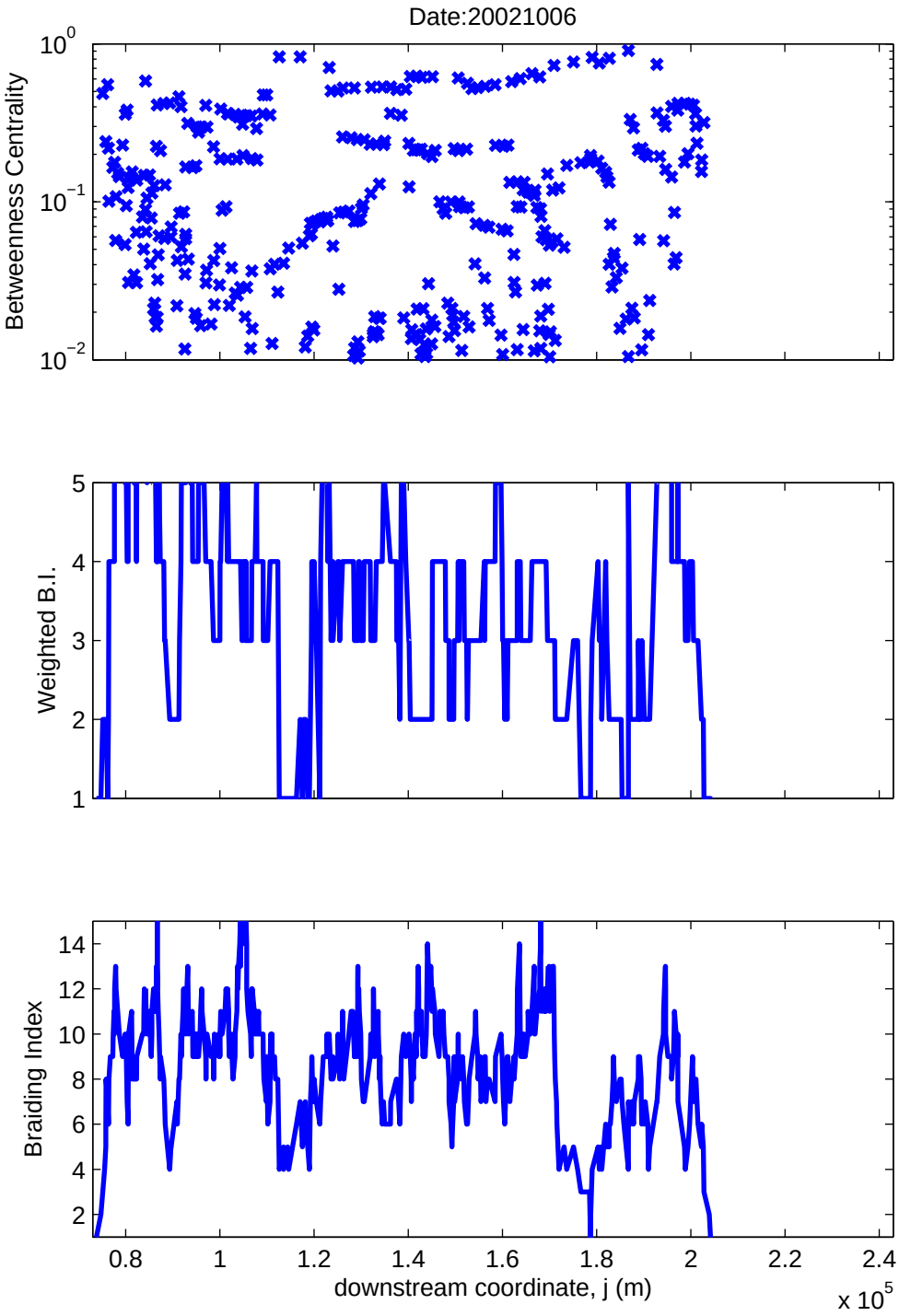

Figure C.9 Braiding index, weighted braiding index and betweenness centrality along the channel network, date: 20021006

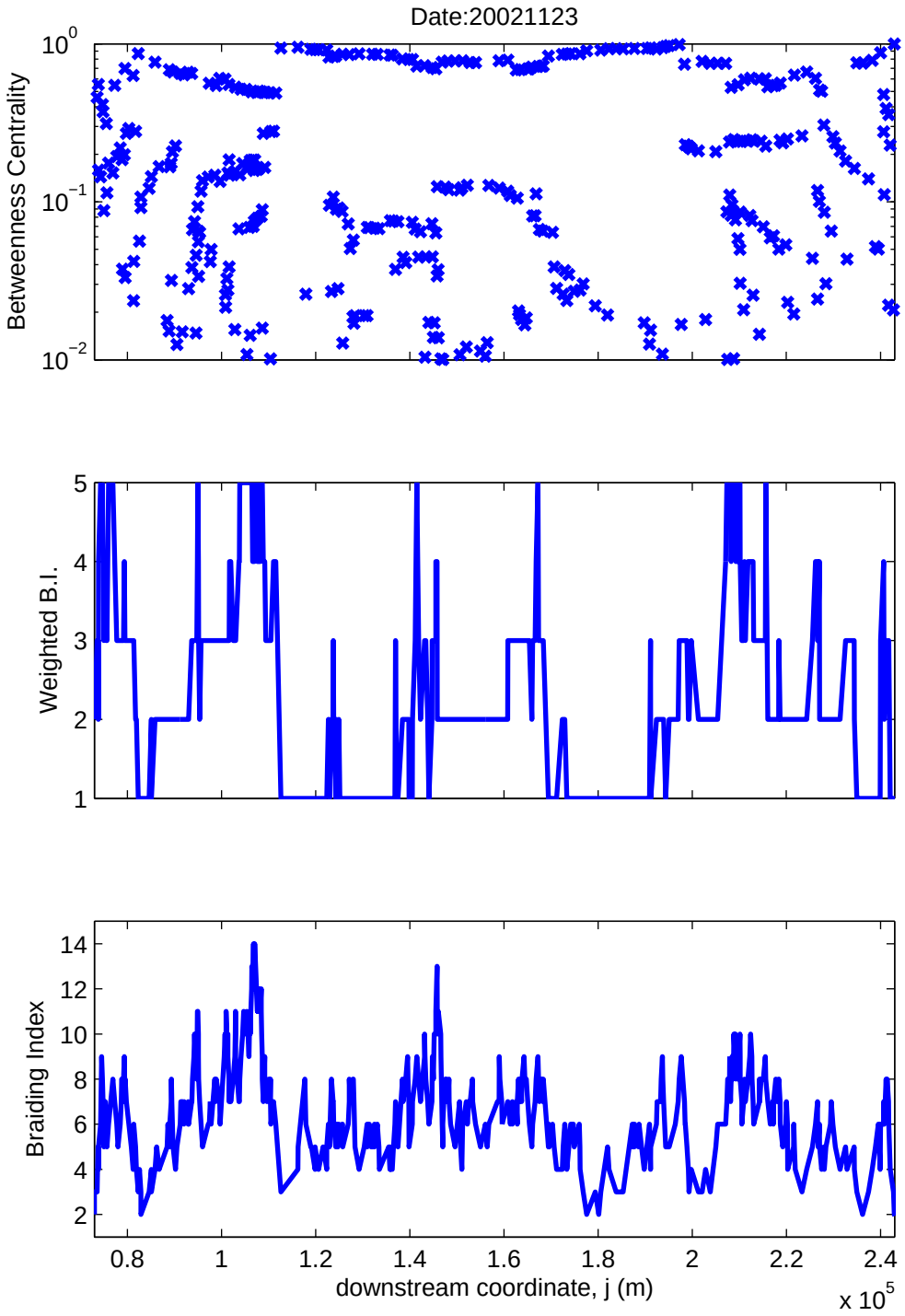

Figure C.10 Braiding Index, Weighted Braiding Index and Betweenness centrality along the channel network, date: 20021123

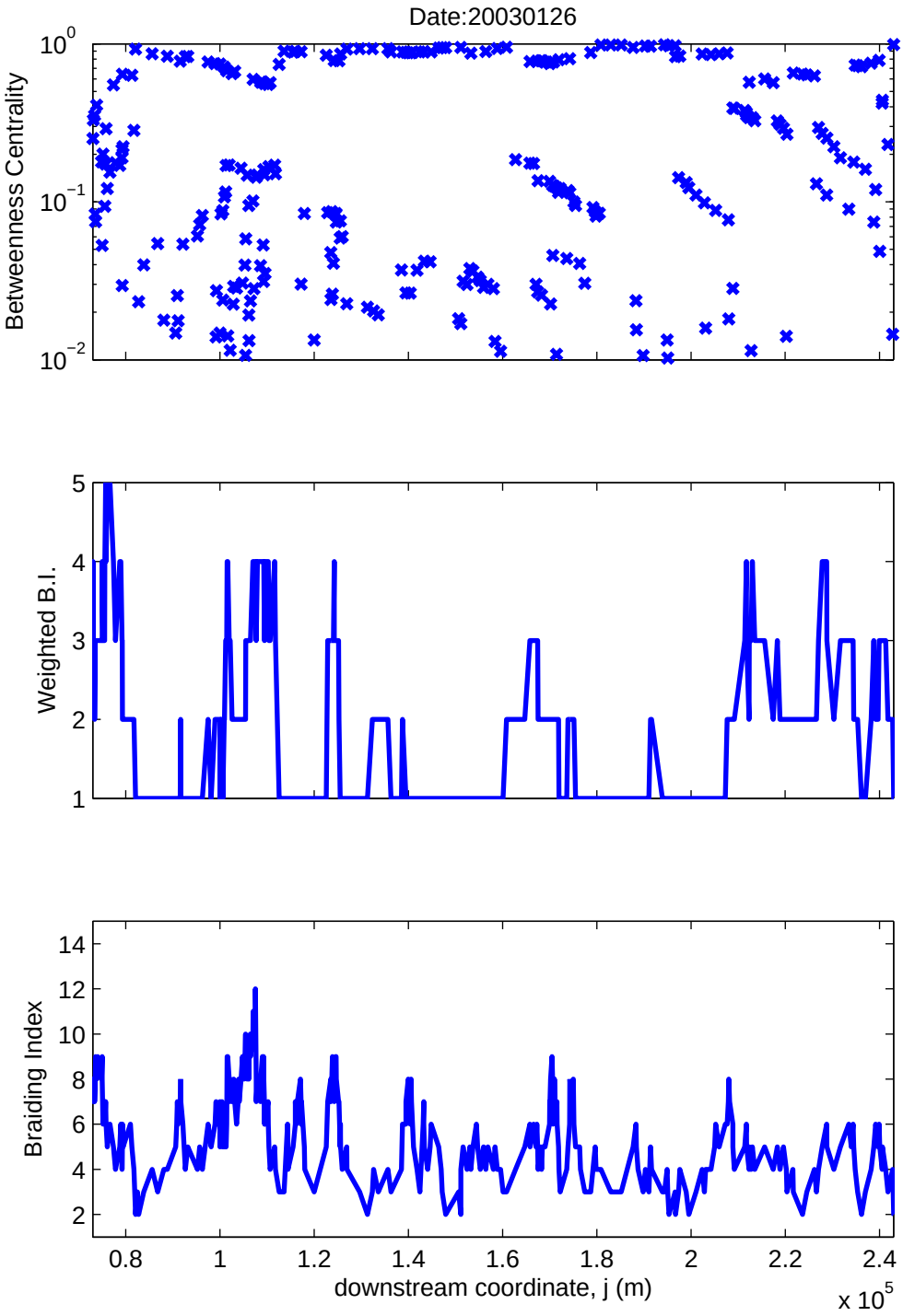

Figure C.11 Braiding index, weighted braiding index and betweenness centrality along the channel network, date: 20030126

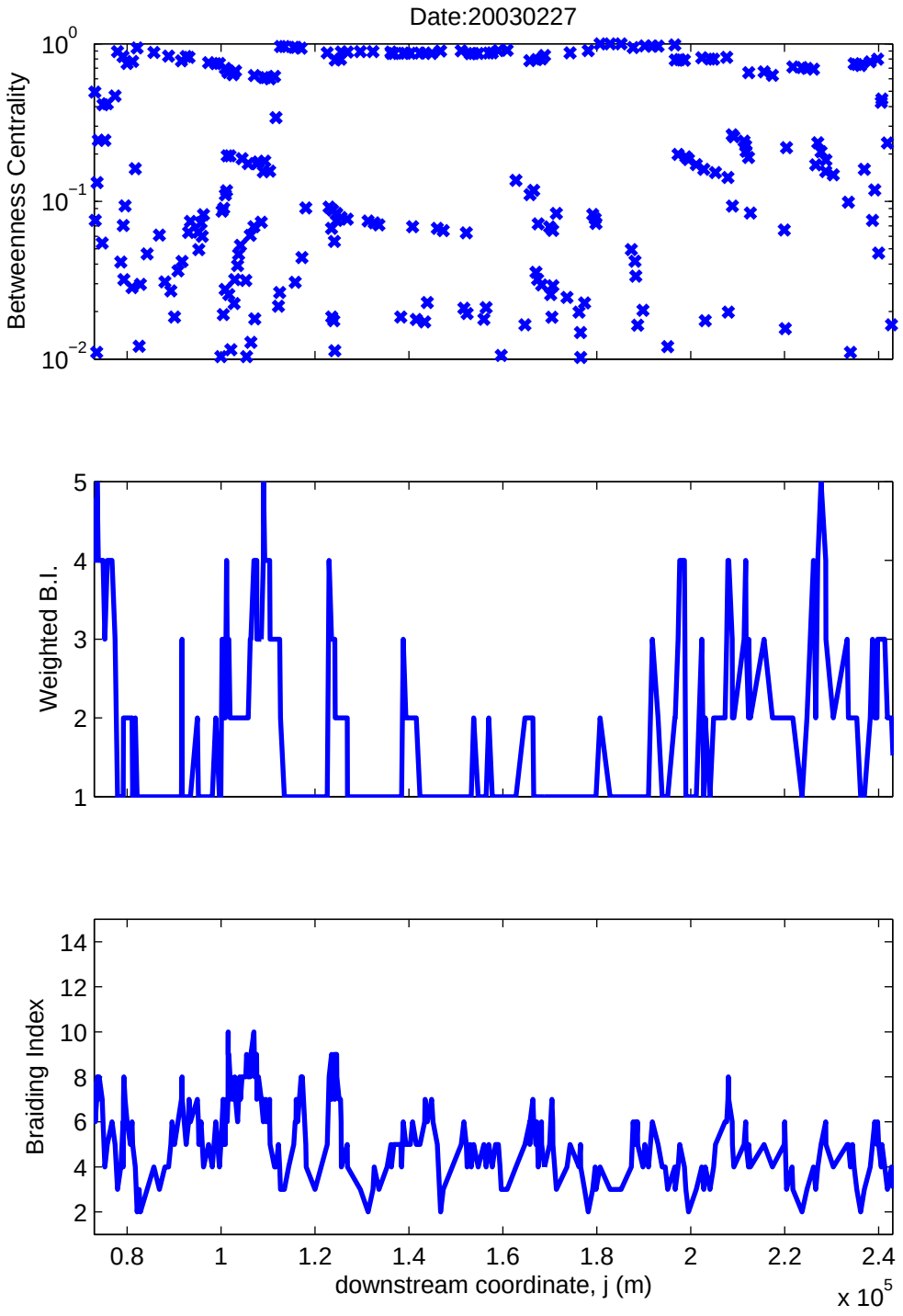

Figure C.12 Braiding index, weighted braiding index and betweenness centrality along the channel network, date: 20030227

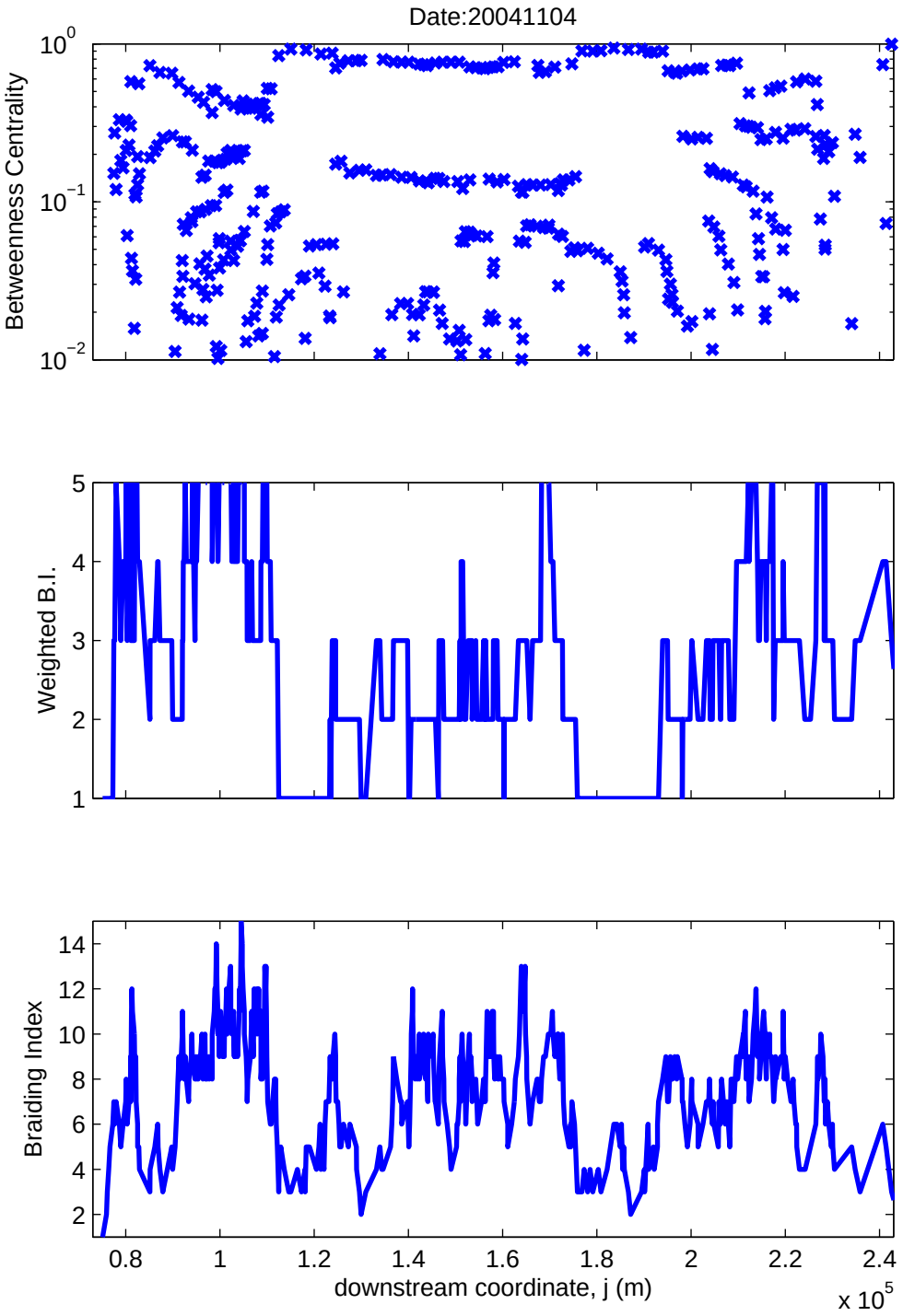

Figure C.13 Braiding index, weighted braiding index and betweenness centrality along the channel network, date: 20041104

Appendix D | Maps of satellite images

If this appendix is not available, contact the author. The appendix is also available on the accompanying hard disk.

Appendix E | Maps of classified images

If this appendix is not available, contact the author. The appendix is also available on the accompanying hard disk.

Appendix F | Maps of channel pixels and centrelines

If this appendix is not available, contact the author. The appendix is also available on the accompanying hard disk.